A fluorescence anisotropy-based assay for determining the activity of tissue transglutaminase

Originally published:

February 2016

Amino Acids 49(2017)3, 567-583

DOI: https://doi.org/10.1007/s00726-016-2192-5

A fluorescence anisotropy-based assay for determining the activity of tissue transglutaminase

Christoph Hauser, Robert Wodtke, Reik Löser, Markus Pietsch

Christoph Hauser, Markus Pietsch
Center of Pharmacology, Medical Faculty, University of Cologne, Gleueler Str. 24, D-50931 Cologne, Germany

Robert Wodtke, Reik Löser
Helmholtz-Zentrum Dresden-Rossendorf, Institute of Radiopharmaceutical Cancer Research, Bautzner Landstr. 400, D-01328 Dresden, Germany
and
Department of Chemistry and Food Chemistry, Technical University Dresden, Mommsenstraße 4, D-01062 Dresden, Germany

Christoph Hauser and Robert Wodtke as well as Reik Löser and Markus Pietsch contributed equally to this study.

Corresponding authors
Dr. Markus Pietsch, Center of Pharmacology, Medical Faculty, University of Cologne, Gleueler Str. 24, D-50931 Cologne, Germany, Phone: +49 (0)221 478-97737, Fax: +49 (0)221 478-5022, E-Mail: markus.pietsch@uk-koeln.de

Dr. Reik Löser, Helmholtz-Zentrum Dresden-Rossendorf, Institute of Radiopharmaceutical Cancer Research, Bautzner Landstr. 400, D-01328 Dresden, Germany, Phone: +49 (0)351 260-3658, Fax: +49 (0)351 260-2915, E-Mail: r.loeser@hzdr.de

Abstract

Tissue transglutaminase (TGase 2) is the most abundantly expressed enzyme of the transglutaminase family and involved in a large variety of pathological processes, such as neurodegenerative diseases, disorders related to autoimmunity and inflammation as well as tumor growth, progression and metastasis. As a result, TGase 2 represents an attractive target for drug discovery and development, which requires assays that allow for the characterization of modulating agents and are appropriate for high-throughput screening. Herein, we report a fluorescence anisotropy-based approach for the determination of TGase 2's transamidase activity, following the time-dependent increase in fluorescence anisotropy due to the enzyme-catalyzed incorporation of fluorescein- and rhodamine B-conjugated cadaverines **1**-**3** (acyl acceptor substrates) into *N*,*N*-dimethylated casein (acyl donor substrate). These cadaverine derivatives **1**-**3** were obtained by solid-phase synthesis. To allow efficient conjugation of the rhodamine B moiety, different linkers providing secondary amine functions, such as sarcosyl and isonipecotyl, were introduced between the cadaverine and xanthenyl entities in compounds **2** and **3**, respectively, with acyl acceptor **3** showing the most optimal substrate properties of the compounds investigated. The assay was validated for the search of both irreversible and reversible TGase 2 inhibitors using the inactivators iodoacetamide and a recently published L-lysine-derived acrylamide and the allosteric binder GTP, respectively. In addition, the fluorescence anisotropy-based method was proven to be suitable for high-throughput screening (Z' factor of 0.86) and represents a non-radioactive and highly sensitive assay for determining the active TGase 2 concentration.

Keywords

Active-site titration, Cadaverine, Enzyme inhibition, Fluorescent labeling, Transglutaminases, Xanthene dyes

Abbreviations

ANOVA	analysis of variance
BHNA	α-bromo-4-hydroxy-3-nitroacetophenone
BFP	blue fluorescent protein
2-ClTrtCl	2-chlorotrityl chloride
DIPEA	*N*,*N*-diisopropylethylamine
DMC	*N*,*N*-dimethylated casein
DMF	*N*,*N*-dimethylformamide
DMSO	dimethyl sulfoxide
DTT	1,4-dithio-D-threitol
EDTA	ethylenediaminetetraacetic acid
ESI-MS	electrospray ionization mass spectrometry
E_{tot}	theoretical total enzyme concentration
FA	fluorescence anisotropy
FITC	fluorescein-5-isothiocyanate
Fmoc	9-fluorenylmethyloxycarbonyl
FRET	Förster resonance energy transfer
GFP	green fluorescent protein
GMP-PNP	guanosine 5′-[β,γ-imido]triphosphate

gp	guinea pig
GTP	guanosine triphosphate
HATU	1-[bis(dimethylamino)methylene]-1*H*-1,2,3-triazolo[4,5-*b*]pyridinium 3-oxid hexafluorophosphate
HEPES	(4-(2-hydroxyethyl)-1-piperazineethanesulfonic acid
HTS	high-throughput screening
Inp	isonipecotyl
KXD	(*S*)-tert-butyl 6-amino-1-(2-(5-(dimethylamino)naphthalene-1-sulfonamido) ethylamino)-1-oxohexan-2-ylcarbamate (Boc-Lys-en-dansyl)
L-PACK	*N*-(2-hydroxy-5-nitrophenylacetyl)-L-2-amino-4-oxo-5-chloropentanoate
MOPS	3-(*N*-morpholino)propanesulfonic acid
NMR	nuclear magnetic resonance
PP	polypropylene
PyBOP	benzotriazol-1-yl-oxytripyrrolidinophosphonium hexafluorophosphate
RFU	relative fluorescence units
RP-HPLC	reversed-phase high-pressure liquid chromatography
Sar	sarcosyl
SD	standard deviation
SEM	standard error of the mean
SNAP-25	25 kDa synaptosome-associated protein
TEA	triethylamine
TES	2-[[1,3-dihydroxy-2-(hydroxymethyl)propan-2-yl]amino]ethanesulfonic acid
TFA	trifluoroacetic acid
TGase	transglutaminase
TMS	tetramethylsilane
UV	ultraviolet

Introduction

Tissue transglutaminase, also known as transglutaminase 2 (TGase 2, EC 2.3.2.13), is an abundantly expressed enzyme whose catalytic activities on a broad range of substrates and non-catalytic interactions with protein binding partners result in a large variety of physiological and pathological implications. Among the most prominent disorders negatively influenced by TGase 2 are celiac disease, several neurodegenerative diseases (such as Alzheimer's disease, Parkinson's disease and Huntington's disease), tumor growth, progression and metastasis, as well as cataractogenesis (Agnihotri et al. 2013; Beninati et al. 2013; Lentini et al. 2013; Pietsch et al. 2013; Odii and Coussons 2014; Ientile et al. 2015; Kanchan et al. 2015). The involvement of TGase 2 in these pathological processes renders the enzyme an attractive target for the development of inhibitors as potential therapeutic agents (Badarau et al. 2013; Keillor et al. 2015), with screening of compound libraries representing one approach for initial lead identification, as recently demonstrated (Case and Stein 2007; Schaertl et al. 2010).

TGase 2 exhibits a variety of enzymatic activities, such as those of a transamidase, a hydrolase and a GTPase, with the former two activities (Ca^{2+}-dependent) being often applied in the identification/characterization of inhibitors (Lai et al. 1998; Pietsch et al. 2013; Keillor et al. 2014). Both transamidation and hydrolysis of acyl donor substrates follow an acylation-deacylation mechanism accompanied by the formation of an acyl enzyme which undergoes reaction with acyl acceptor substrates, such as amines and water, respectively (Keillor et al. 2014). We have recently surveyed the majority of reported assays to quantify the hydrolytic and transamidase activities of the transglutaminases TGase 2 and factor XIIIa (Pietsch et al. 2013). So far only very few assays have been described using the method of fluorescence polarization (fluorescence anisotropy, FA) to determine the enzymes' transamidase activity by measuring the increase in anisotropy over time (Yamada and Meguro 1977; Kongsbak et al.

1999; Kenniston et al. 2013). In addition, this technique has been applied by Lorand and coworkers to investigate transglutaminase regarding its binding to fibronectin (fragments) (Radek et al. 1993; Jeong et al. 1995) and interaction with guanine nucleotides (Murthy and Lorand 2000) by means of fluorescently labeled ligands.

Monitoring the action of target enzymes by following the change in FA over time is an established technique to quantify the enzymes' activity and inhibition as reported by several groups (Sem and McNeeley 1999; Li et al. 2000; Simeonov et al. 2002; Blommel and Fox 2005; Nakayama et al. 2006; Cleemann and Karuso 2008; Shapiro et al. 2014). Applying the FA as readout allows for homogeneous assays, which is advantageous for high-throughput screening (HTS) of compound libraries (Jameson and Ross 2010; Lea and Simeonov 2011). However, interferences occur due to autofluorescence and light scattering, which can be counteracted by kinetic reads and the usage of red-shifted dyes as fluorescent probes (Owicki 2000; Lea and Simeonov 2011). Fluorophores commonly used as probes in biological systems have recently been reviewed by Lavis and Raines (Lavis and Raines 2014) and Grimm et al. (Grimm et al. 2013), with fluorescein being one of the most frequently applied dyes. However, fluorescein is prone to photodegradation, interference by autofluorescence and fluorescent compounds in libraries, and both its structure and spectral properties considerably depend on the pH (Owicki 2000; Simeonov et al. 2008; Jameson and Ross 2010). To circumvent these drawbacks, the amino analogues of fluorescein, i.e. rhodamines, can be applied, which are characterized by a lower pH-sensitivity, an increased photostability, and more red-shifted absorption and emission spectra reducing measuring artifacts when screening compound libraries (Simeonov et al. 2008; Beija et al. 2009; Grimm et al. 2013; Lavis and Raines 2014). Among the commercially available dyes of the rhodamine family, rhodamine B is one of the most often utilized derivatives due to its relatively low price (Beija et al. 2009).

We have developed a kinetic FA-based assay to characterize TGase's 2 transamidase activity and its interaction with three established inhibitors (Fig. 1) by using *N*,*N*-dimethylated casein (DMC) and three synthesized cadaverine derivatives labeled either with fluorescein [FITC cadaverine (**1**) (Lorand et al. 1983)] or rhodamine B (compounds **2** and **3**). Varying the linker between rhodamine B and cadaverine, we were able to optimize the substrate properties of the acyl acceptor and prove the suitability of the FA assay for HTS. Kinetic measurements of FA instead of fluorescence intensity allowed for the development of a rapid and homogeneous assay that does not require separation of fluorescent substrates and products. In addition, choosing FA as readout resulted in low background noise and offered the advantage of being independent of changes in the spectral properties of the dyes during protein binding (Kongsbak et al. 1999). TGase 2 from guinea pig liver was chosen as it is a cost-effective alternative to the human enzyme, with the two TGases following "identical kinetic mechanisms with nearly identical kinetic parameters for the mechanistic rate constants" (Case and Stein 2003) when assayed with the established substrates DMC and dansyl cadaverine. Moreover, fluorescently labeled cadaverines and casein have already been proven to be applicable for FA measurements on factor XIIIa (Yamada and Meguro 1977) and TGase from *Phytophthora cactorum* (Kongsbak et al. 1999), thus, these results represent a verified basis for developing the new assay.

Material and methods

Material

TGase 2 isolated from guinea pig liver (product number: T006) and guinea pig liver TGase 2 recombinantly produced in *Escherichia coli* (product number: T039) were purchased from Zedira, Darmstadt, Germany. DMC from bovine milk (Sigma-Aldrich, product number: C9801, Taufkirchen, Germany), dimethyl sulfoxide (DMSO, Sigma-Aldrich, product number: 41647, Taufkirchen, Germany), rhodamine B (Merck, product number: 107599, Darmstadt, Germany), FITC isomer I (Alfa Aesar, product number: L09319, Karlsruhe, Germany), 1,5-diaminopentane (cadaverine, Acros Organics, product number: 112320050, New Jersey, USA), Fmoc-Sar-OH (Merck Novabiochem, product number: 8520550005, Hohenbrunn, Germany), Fmoc-Inp-OH (Iris Biotech, product number: FAA13450005, Marktredwitz, Germany), guanosine triphosphate disodium salt × 3 H_2O (GTP, Roth, product number: K056.1, Karlsruhe, Germany), and iodoacetamide (Fluka, product number: 57670, Steinheim, Germany) were commercially obtained. Inhibitor **4** was prepared as trifluoroacetate salt following the method of Wityak et al. (Wityak et al. 2012) with some modifications. Nuclear magnetic resonance spectra were recorded on a Varian Unity 400 MHz or an Agilent Technologies 400 MR spectrometer. The NMR machines were operated by the VnmrJ software (version 4.2). 2D NMR spectra were recorded using pulse sequences and parameters as preimplemented in the software. COSY and HSQC spectra were recorded in gradient mode, mixing time (duration of spin lock) for TOCSY was 120 ms. Spectra were processed by using MestreNova (version 6.1.1-6384) (Cobas et al. 2010). NMR chemical shifts were referenced to the residual solvent resonances relative to tetramethylsilane (TMS). Mass spectra (ESI) were obtained on a Micromass Quattro LC or a Waters Xevo TQ-S mass spectrometer each driven by the Mass Lynx software.

Chromatography

Analytical and preparative HPLC of compounds **1-3** were performed on a Varian Prepstar system equipped with UV detector (Prostar, Varian) and automatic fraction collector Foxy 200. Two Microsorb C18 60-8 columns (Varian Dynamax 250 × 4.6 mm and 250 × 21.4 mm) were used as the stationary phases for analytical and preparative HPLC, respectively. A binary gradient system of 0.1% CF_3COOH/water (solvent A) and 0.1% CF_3COOH/CH_3CN (solvent B) served as the eluent at flow rates of 1 mL/min or 10 mL/min in analytical and preparative mode, respectively. Regarding analytical HPLC, the programme for elution of compounds was as follows: 0-5 min 95% A, 5-25 min gradient to 95% B, 25-30 min 95% B, 30-31 min gradient back to 95 % A, 31-35 min 95% A. Regarding preparative HPLC, the conditions for the gradient elution were as follows: 0-7 min 90% A, 7-22 min gradient to 80% B, 22-30 min 80% B, 30-31 min gradient back to 90 % A, 31-35 min 90% A.

Synthesis of the cadaverine derivatives **1-3**

Loading of cadaverine onto 2-ClTrtCl resin. The synthesis was accomplished according to Egner et al. (Egner et al. 1995). A solution of cadaverine (526 µL, 4.48 mmol, 4 equiv.) in CH_2Cl_2 (5 mL) was added to the pre-swollen (5 mL, CH_2Cl_2, 30 min) 2-ClTrtCl resin (0.7 g, 1.12 mmol, 1 equiv., 1.6 mmol/g) in a polypropylene (PP) filter vessel. The PP filter vessel was sealed and agitated for 17 h. Afterwards, the resin was successively washed with DMF (4 mL, 4×1 min), CH_2Cl_2 (4 mL, 4×1 min), CH_2Cl_2/CH_3OH/DIPEA (17/1/2, 4 mL, 3×2 min), CH_3OH (4 mL, 4×1 min), TEA/DMF (1/4, 4 mL, 3×1 min), CH_3OH (4 mL, 4×1 min) and finally with CH_2Cl_2 (4 mL, 4×1 min) again. The resin was dried in vacuo overnight. The loading yields were quantitative as confirmed by gravimetrical determination according to Bernecker et al. (Bernecker et al. 2010) using the following equation: B (mol/g)

= $(m_2-m_1)/((MW-36.461)*m_2)$, with m_1 and m_2 being the weights of the unloaded and the loaded resin in g, respectively, and MW being the molecular weight of cadaverine in g/mol. The value of the loading yield was B = 1.5 mmol/g.

Coupling of fluorescein-5-isothiocyanate. The cadaverine-loaded resin (0.66 mmol cadaverine, 1 equiv.) was swollen in DMF (5 mL) for 30 min. After filtering, a solution of fluorescein-5-isothiocyanate (FITC isomer I; 256 mg, 0.66 mmol, 1 equiv.) and TEA (184 µL, 1.32 mmol, 2 equiv.) in DMF (4 mL) was added to the resin. The resulting suspension was sealed and agitated for 8 h in the dark. Finally, the resin was washed with DMF (4 mL, 4×1 min) and CH_2Cl_2 (4 mL, 4×1 min) and was dried in vacuo overnight.

Coupling of Fmoc-Sar-OH and Fmoc-Inp-OH with subsequent acetylation. A solution of Fmoc-Sar-OH (311 mg, 1.0 mmol, 2 equiv.) or Fmoc-Inp-OH (351 mg, 1.0 mmol, 2 equiv.) and DIPEA (348 µL, 2.0 mmol, 4 equiv.) in DMF (4 mL) was added to the pre-swollen (5 mL, DMF, 30 min) cadaverine-loaded resin (0.5 mmol cadaverine, 1 equiv.). After 1 min, PyBOP (520 mg, 1.0 mmol, 2 equiv.) was added and the resulting suspension was sealed and agitated for 5 h; afterwards, the resin was washed with DMF (4 mL, 4×1 min). Subsequent acetylation of unreacted cadaverine was performed by treatment of the resin with a 0.5 M solution of acetic anhydride/DIPEA in DMF (5 mL, 1×3 min). Finally, the resin was washed with DMF (4 mL, 4×1 min) and CH_2Cl_2 (4 mL, 4×1 min) and was dried in vacuo overnight.

Removal of Fmoc protecting group. After coupling of Fmoc-Sar-OH or Fmoc-Inp-OH, the respective resin was swollen in DMF (5 mL) for 30 min. The Fmoc group was removed by repetitive treatment with 20% piperidine in DMF (5 mL, 3×10 min, 1×15 min). Then, the

resin was washed with DMF (4 mL, 4×1 min) and CH_2Cl_2 (4 mL, 4×1 min) and was dried in vacuo overnight.

Coupling of rhodamine B. To a solution of rhodamine B (479 mg, 1.0 mmol, 2 equiv.) and DIPEA (348 µL, 2.0 mmol, 4 equiv.) in DMF was added HATU (380 mg, 1.0 mmol, 2 equiv.) and the resulting mixture was stirred for 15 min (pre-activation) in the dark. Afterwards, this solution was added to the pre-swollen (5 mL, DMF, 30 min) resin (initially 0.5 mmol cadaverine, 1 equiv.) and the resulting suspension was sealed and agitated for 5 h in the dark. Finally, the resin was extensively washed with DMF (6 mL, 4×1 min) and CH_2Cl_2 (4 mL, 6×1 min) and was dried in vacuo overnight.

Cleavage of the resin-bound xanthene dye-cadaverine conjugates. The dry resin was suspended in 5 mL of a solution of TFA/TES/H_2O (95/2.5/2.5) for 2 h. After filtering, the resin was washed with TFA (2×5 mL) and the combined filtrates were evaporated in a N_2 stream. The oily residues were purified by RP-HPLC, the product-containing fractions were pooled, concentrated under reduced pressure on a rotary evaporator and lyophilized to obtain the final products **1**-**3**.

Analytical data of the cadaverine derivatives **1**-**3**

*5'-((5-Aminopentyl)thioureidyl)fluorescein × TFA (**1**)*

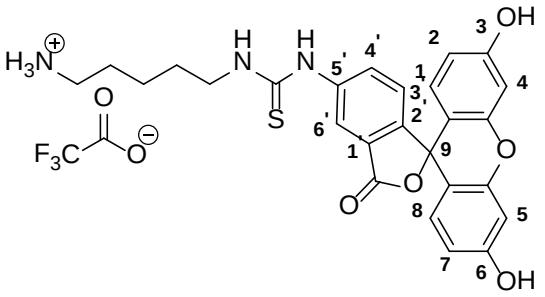

The resin-bound cadaverine (0.66 mmol) yielded 205 mg (0.34 mmol, 52%) of compound **1** as an orange voluminous solid; RP-HPLC analysis: t_R = 18.3 min. The NMR signals were assigned on the basis of 2D experiments (COSY and HSQC) and based on published data for the fluorescein moiety (Anthoni et al. 1995). ^{1}H-NMR (400 MHz, DMSO-d_6): δ = 10.06 (s, 1H, phenyl-NH), 8.27 (t, ^3J = 5.2 Hz, 1H, CH_2NH), 8.23 (s, 1H, H–6'), 7.73 (d, ^3J = 7.4 Hz, 1H, H–4'), 7.68 (broad s, 3H, NH_3^+), 7.18 (d, ^3J = 8.3 Hz, 1H, H–3'), 6.68 (d, ^4J = 2.2 Hz, 2H, H–4,5), 6.62–6.54 (m, 4H, H–1,2,7,8), 3.56–3.47 (m, 2H, CH_2NH), 2.86–2.75 (m, 2H, $CH_2NH_3^+$), 1.64–1.52 (m, 4H, H–2,4 of cadaverine), 1.42–1.32 (m, 2H, H–3 of cadaverine); ^{13}C-NMR (101 MHz, DMSO-d_6): δ = 180.44 (CS), 168.54 (CO), 159.49 (C–3,6), 158.31 (q, $^2J_{C,F}$ = 34.4 Hz (CO TFA), 151.87 (C–4a,5a), 147.03, 141.44, 129.42 (C–4'), 128.99 (C–1,8), 126.47, 124.02 (C–3'), 116.33 (C–6'), 112.58 (C–2,7), 109.71 (C–1a,8a), 102.24 (C–4,5), 83.12 (C–9), 43.54 (CH_2NH), 38.80 ($CH_2NH_3^+$), 27.79, 26.72, 23.23 (C–3 of cadaverine); ^{19}F-NMR (376 MHz, DMSO-d_6): δ = -74.34 (s, CF_3); ESI-MS (ESI+) m/z: calc. for $C_{26}H_{26}N_3O_5S$, $[M+H]^+$, 492.16, found 492.1.

*2'-((5-Aminopentyl)sarcosyl)rhodamine B × 2 TFA (**2**)*

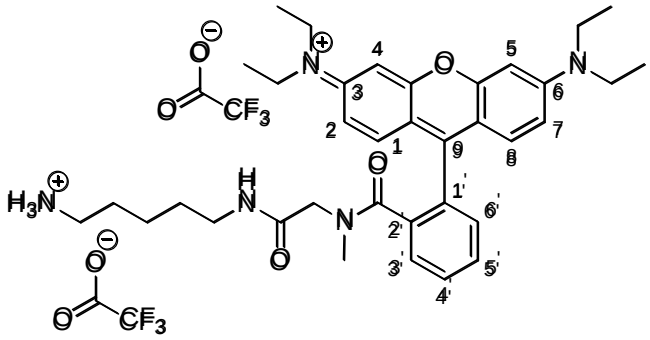

The resin-bound cadaverine (0.5 mmol) yielded 94 mg (0.11 mmol, 23%) of compound **2** as a red-purple oily solid; RP-HPLC analysis: t_R = 20.7 min; mixture of sarcosine s-*trans*/s-*cis* isomers (ratio 6 : 4). The NMR signals were assigned on the basis of 2D experiments (TOCSY and HSQC) and based on published data for the rhodamine moiety (Ramos et al. 2000). When possible, chemical shifts were assigned to the major (A) and minor (B) isomer: ^{1}H-NMR (400 MHz, DMSO-d_6): δ = 8.06 (t, ^3J = 5.7 Hz, 0.4H, NH of B), 7.82–7.63 (m, 6.6H, NH_3^+, 3×H_{Phenyl}, NH of A), 7.54–7.48 (m, 1H, H_{Phenyl}), 7.17–7.04 (m, 4H, H–1,2,7,8), 6.95 (d, ^4J = 2.3 Hz, 0.8H, H–4,5 of B), 6.94 (d, ^4J = 2.3 Hz, 1.2H, H–4,5 of A), 3.84 (s, 0.8H, CH_2 of sarcosine for B), 3.72–3.59 (m, 9.2H, 4×CH_2 of rhodamine B, CH_2 of sarcosine for A), 3.11-3.04 (m, 0.8H, CH_2NH of B), 2.94–2.87 (m, 1.2H, CH_2NH of A), 2.85 (s, 1.8H, CH_3 of sarcosine for A), 2.82–2.68 (m, 2H, C$H_2NH_3^+$), 2.58 (s, 1.2H, CH_3 of sarcosine for B), 1.60–1.16 (m, 18H, 4×CH_3 of rhodamine B, H–2,3,4 of cadaverine); ^{13}C-NMR (101 MHz, DMSO-d_6): δ = 168.28 (CO of amide for B), 168.05 (CO of amide for A), 167.37 (CO of amide for B), 166.94 (CO of amide for A), 157.99 (q, $^2J_{C,F}$ = 31.6 Hz, CO of TFA), 157.23 (A), 157.09 (B), 155.59 (B), 155.25 (A), 155.12, 135.80 (A), 135.69 (B), 131.85 (C–1,8 of A), 131.78 (C–1,8 of B), 130.51, 130.40, 130.23, 130.18, 129.85, 129.66, 129.58, 129.47, 127.41 (CH_{Phenyl} of A), 127.02 (CH_{Phenyl} of B), 113.99 (C–2,7), 113.15 (C–8a,9a of A), 113.09 (C–8a,9a of B), 95.86 (C–4,5 of A), 95.76 (C–4,5 of B), 53.50 (CH_2 of

sarcosine for B), 49.30 (CH_2 of sarcosine for A), 45.31 (4×CH_2 of rhodamine B), 38.73 ($CH_2NH_3^+$ for B), 38.70 ($CH_2NH_3^+$ for A), 38.44 (CH_3 of sarcosine for A), 38.32 (CH_2NH of B), 38.14 (CH_2NH of A), 33.32 (CH_3 of sarcosine for B), 28.46 (C–2 of cadaverine for B), 28.40 (C–2 of cadaverine for A), 26.62 (C–4 of cadaverine), 23.15 (C–3 of cadaverine), 12.44 (4×CH_3 of rhodamine B).; ^{19}F-NMR (376 MHz, DMSO-d_6): δ = -74.24 (s, CF_3); ESI-MS (ESI+) m/z: calc. for $C_{36}H_{48}N_5O_3$, $[M]^+$, 598.38, found 598.2.

2'-((5-Aminopentyl)isonipecotyl)rhodamine B × 2 TFA ***(3)***

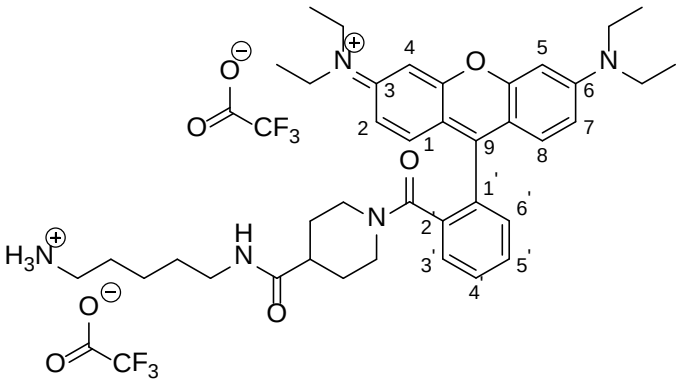

The resin-bound cadaverine (1.0 mmol) yielded 211 mg (0.24 mmol, 24%) of compound **3** as a red-purple oily solid; RP-HPLC analysis: t_R = 21.5 min. The NMR signals were assigned on the basis of 2D experiments (COSY, TOCSY and HSQC) and based on published data for the rhodamine moiety (Ramos et al. 2000). ^{1}H-NMR (400 MHz, DMSO-d_6): δ = 7.77–7.60 (m, 7H, NH_3^+, NH, 3×H_{Phenyl}), 7.54–7.49 (m, 1H, H_{Phenyl}), 7.21–7.03 (m, 4H, H–1,2,7,8), 6.95 (d, ^4J = 2.1 Hz, 2H, H–4,5), 4.08 (psd, J = 11.6 Hz, 1H, CHN of Inp), 3.76 (psd, J = 13.1 Hz, 1H, CHN of Inp), 3.66 (q, ^3J = 7.1 Hz, 8H, 4×CH_2 of rhodamine B), 3.07–2.91 (m, 3H, CH_2NH, CHN of Inp), 2.80–2.69 (m, 2H, C$H_2NH_3^+$), 2.51–2.45 (m, 1H, CHN of Inp), 2.30–2.19 (m, 1H, CH of Inp), 1.62–1.53 (m, 2H, CH_2 of Inp), 1.53–1.45 (m, 2H, H–4 of cadaverine), 1.44–1.31 (m, 3H, H–2 of cadaverine, CH*H* of Inp), 1.31–1.16 (m, 15H, 4×CH_3, H–3 of cadaverine, C*H*H of Inp); ^{13}C-NMR (101 MHz, DMSO-d_6): δ = 173.30

(CO of amide), 166.17 (CO of amide), 157.97 (q, $^{2}J_{C,F}$ = 33.9 Hz, CO of TFA), 157.02, 155.74, 155.08, 135.78, 131.77 (C–1,8), 130.50, 130.40 (CH_{Phenyl}), 129.76 (CH_{Phenyl}), 129.48 (CH_{Phenyl}), 127.20 (CH_{Phenyl}), 114.37 (C–2,7), 112.96 (C–8a,9a), 95.88 (C–4,5), 46.57 (CH_2N of Inp), 45.34 (4×CH_2 of rhodamine B), 41.33 (CH of Inp), 40.62 (CH_2N of Inp), 38.73 ($CH_2NH_3^+$), 38.06 (CH_2NH), 28.53 (C–2 of cadaverine), 28.47 (CH_2 of Inp), 28.03 (CH_2 of Inp), 26.65 (C–4 of cadaverine), 23.15 (C–3 of cadaverine), 12.43 (4×CH_3); ^{19}F-NMR (376 MHz, DMSO-d_6): δ = -74.22 (s, CF_3); ESI-MS (ESI+) m/z: calc. for $C_{39}H_{52}N_5O_3$, $[M]^+$, 638.41, found 638.3.

FA-based TGase 2 assay

The FA assay and fluorescence measurements were performed at 30 °C in black BRANDplates pureGrade 96-well plates with F-bottom wells (Brand, Wertheim, Germany) using BioTek Synergy 2 and BioTek Synergy 4 multimode microplate readers with the software Gen 5 version 1.11.5 (Bad Friedrichshall, Germany). Absorption and emission spectra of compounds **1**-**3**, fluorescein, and rhodamine B (Online Resource Fig. S1) were measured at the BioTek Synergy 4 equipped with a BioTek BioCell 1 cm Quartz Vessel. Experiments were done at excitation wavelengths of 485 nm (**1**) and 540 nm (**2**, **3**) and emission wavelengths of 528 nm (**1**) and 620 nm (**2**, **3**), respectively. The FA (r) was calculated by the Gen 5 software from the measured parallel and perpendicular fluorescence intensities ($I_{\parallel}$ and $I_{\perp}$, respectively) according to the equation $r = (I_{\parallel} - G \times I_{\perp}) / (I_{\parallel} + 2G \times I_{\perp})$ using a G factor of 0.87 (preset value) to correct "the intrinsic bias of the detector system's response for one plane of polarized light over the other" (Reindl et al. 2009). All further data analysis including calculation of rates by linear regression of the FA over time, curve fitting, and statistics were conducted with GraphPad Prism version 5.04 for Windows (GraphPad Software, San Diego, CA, USA). Values are given as mean value ± standard error of the

means (SEM), with *n* being the number of experiments done, or as mean value ± standard deviation (SD).

The assay buffer was 100 mM MOPS pH 8.0 containing 3 mM $CaCl_2$ and 50 µM EDTA (pre-heated to 30 °C). Inhibition of TGase 2 by GTP was measured with pre-heated assay buffer (30 °C) consisting of 50 mM HEPES pH 7.4, 500 mM NaCl, 1 mM $CaCl_2$, 2 mM $MgCl_2$ (Case et al. 2005). TGase 2 stock (0.5 mg/mL) was prepared in ice-cold 100 mM MOPS with 3 mM $CaCl_2$, 10 mM DTT and 20% (v/v) glycerol (pH 8.0), stored at -80 °C, and freshly diluted (1:5) in the same buffer or HEPES assay buffer containing 22.5 mM DTT (inhibition of TGase 2 by GTP) before each measurement. The acyl donor substrate DMC was dissolved in the respective assay buffer (2.5 mM) and diluted with the same buffer. Stock solutions and dilutions of the acceptor substrates **1** (8.12 mM and 16.2 mM), **2** (16.2 mM), and **3** (16.2 mM) and those of the inhibitors iodoacetamide (50 mM) and compound **4** (10 mM) were prepared in DMSO; GTP (500 mM) was dissolved and diluted in water. All assays were performed in a volume of 200 µL in the presence of 5% (v/v) DMSO. Pre-incubation (30 min) was done in the Synergy 2 / Synergy 4 multimode microplate reader at 30 °C. Dependence of the fluorescence of the cadaverine derivatives on their concentration was investigated in the absence of TGase 2 and DMC by adding 10 µL enzyme buffer, 5 µL DMSO and 5 µL cadaverine derivative (final concentration: 0.406-4.06 µM) to 180 µL assay buffer. Fluorescence was recorded over a period of 20 min and the last value measured was used. For the FA assay, the reaction mixture contained 130 µL assay buffer, 50 µL DMC, 5 µL of stock solution of the respective cadaverine derivative, 5 µL inhibitor or DMSO, and 10 µL TGase 2 or enzyme buffer. Inhibition by GTP was investigated in 125 µL assay buffer, 5 µL DMSO, 50 µL DMC, 5 µL cadaverine derivative, 5 µL GTP or water, and 10 µL TGase 2 or enzyme buffer. Reactions were started after pre-incubation and followed over a period of 15 min.

To investigate the dependence of the enzyme activity on TGase 2 concentration, 10 µM or 30 µM DMC, 0.81 µM cadaverine derivative, and 0-5 µg/mL TGase 2 were used. Reactions were started by addition of DMC.

The Michaelis constant, K_m, the dissociation constant, K_i, and the maximum rate, V_{max}, for the acyl donor substrate DMC were determined in the presence of 0.81 µM cadaverine derivative, 5 µg/mL TGase 2, and 0.3-300 µM DMC. Reactions were started by the addition of TGase 2 or enzyme buffer. K_m, K_i and V_{max} were calculated according to the Michaelis-Menten equation (**1**) or by applying the equation of substrate inhibition (**2**, **3**) (Copeland 2000).

To investigate the influence of various concentrations of the cadaverine derivatives on the reaction rate, 5 µM or 30 µM DMC, 5 µg/mL TGase 2, and 0.000162-4.06 µM cadaverine derivative were used. Reactions were started by addition of DMC. K_m, K_i and V_{max} were calculated according to the equation for substrate inhibition (Copeland 2000). The influence of various concentrations of the cadaverine derivatives on the change in FA (ΔFA) was similarly investigated with 10 µM or 30 µM DMC. Reactions were started by the addition of DMC and the FA was followed over a period of 3 h. Curves obtained in the presence of TGase 2 were analyzed by first order non-linear regression and ΔFA was expressed as difference between the value at t = 0 and the plateau. Reactions in the absence of TGase 2 were analyzed by linear regression and ΔFA was expressed as product of slope and reaction time. The fluorescence of all mixtures was measured after completion of the reaction.

Inhibition of TGase 2 was studied with 10 µM or 30 µM DMC, 0.81 µM cadaverine derivative, 5 µg/mL TGase 2, and 0.0001-10 µM iodoacetamide, 0.001-30 µM compound **4**, and 0.1-3000 µM GTP, respectively. Reactions were started by the addition of DMC. The inhibitor concentration, [I], causing 50% inhibition, IC_{50}, and the Hill slope, n_H, were calculated according to the equation rate = Bottom + ((Top - Bottom) × $[I]^{n_H}$ / ($[I]^{n_H}$ + $IC_{50}{}^{n_H}$)),

with Bottom and Top representing the lower and upper plateaus of the sigmoid dose-response curve, respectively.

Results and Discussion

Synthesis and analytics of the cadaverine derivatives **1**-**3**

Efficient synthetic access to the fluorescent xanthene dye-cadaverine conjugates **1**-**3** is provided by the solid-phase synthesis-based strategy depicted in Scheme 1. NMR and UV/Vis absorption and emission spectra of compounds **1**-**3** can be found in Online Resource Figs. S1-S9.

As alkane diamines tend to react sequentially on both amine groups in acylation-related modifications, with the corresponding mono-functionalized derivatives being difficult to handle due to their hydrophilic character, the 2-chlorotrityl chloride resin was employed to act as both polymeric protecting group and solid support. Loading of cadaverine to the polystyrene-based resin and subsequent capping of the unreacted attachment sites was performed according to published procedures (Egner et al. 1995; Seebach et al. 2008). Reaction of resin-bound cadaverine with commercially available fluorescein isothiocyanate and subsequent cleavage from polymeric support followed by RP-HPLC purification afforded compound **1** in sufficient yield and purity.

To functionalize the cadaverine core unit with fluorescent dyes that emit photons in the red region of the visible electromagnetic spectrum, rhodamine B represents the dye stuff with most favorable cost-to-property ratio as it exhibits advantageous photophysical parameters and high photostability (Beija et al. 2009). Despite the fact that the carboxyl group of rhodamine B can serve as a handle for conjugation to amino groups, the resulting secondary

amides obtained from primary amines will give rise to the formation of non-fluorescent spirolactams (Adamczyk and Grote 2000). For this reason, the connection of the target-interrogating unit and the rhodamine B moiety should be realized via a tertiary amide bond (Nguyen and Francis 2003; Chabot et al. 2010; Brauch et al. 2012; Fürniss et al. 2013; Gomes et al. 2013). To this end, a linker entity that provides a secondary amino group has to be placed between the cadaverine unit and the fluorophore. Therefore, Fmoc-Sar-OH was coupled to the cadaverine-functionalized resin followed by Fmoc-deprotection, each under standard conditions of solid-phase peptide synthesis. Attachment of the rhodamine B moiety was done by activation with the uronium/guanidinium salt-based coupling reagent HATU to ensure sufficient reactivity of its sterically hindered carbonyl group (Kolmakov et al. 2012). In this way, compound **2** was obtained, which was revealed to exist as a mixture of s-*cis* and s-*trans* isomers in solution. This can be deduced from ^{1}H NMR spectra at variable temperatures (Online Resource Fig. S6). At a temperature of 25 °C each rotamer gives a distinct doublet for the protons in position 4 and 5 of the xanthenyl moiety that fuse to a single doublet at higher temperatures; the coalescence temperature is approximately 50 °C (in DMSO-d_6, 400 MHz). To avoid the formation of rotamers, sarcosine as linker entity was replaced by isonipecotic acid to obtain compound **3**. As expected, the ^{1}H NMR spectrum of this rhodamine B cadaverine conjugate (Online Resource Fig. S7) does not include hints for the occurrence of rotamerism; one single doublet is observed for the xanthenyl 4/5 protons. To the best of our knowledge, isonipecotic acid has not been employed as linker for conjugation of rhodamine B so far.

As expected, the shape and intensities of the UV/Vis absorption and emission spectra of both compound **1** and compounds **2** and **3** resemble those of the isolated fluorophores fluorescein and rhodamine B, respectively. Obviously, the maxima for absorption and emission of the rhodamine B-cadaverine conjugates **2** and **3** show identical values and are bathochromically

shifted compared to free rhodamine B, while the value of the Stokes shift did not change upon conjugation (28 nm for rhodamine B, **2** and **3**; Online Resource Fig. S1).

Measurement of fluorescence anisotropy usually requires the use of monochromatic filters for excitation and emission. In the case of this study the preset values were as outlined in the section Materials and Methods. For compounds **2** and **3**, the filter wavelengths (540 nm and 620 nm for excitation and emission, respectively) were more distant from the maxima (567 nm and 595 nm) than in the case of the fluorescein conjugate **1** (filter wavelengths 485/528 nm and maxima at 494/522 nm for excitation/emission, respectively). Consequently, the fluorescence intensities of **2** and **3** are lower compared to **1** when measured in filter mode (Online Resource Fig. S10). However, this fact did not impede their use as transglutaminase 2 substrates.

Establishment of the new FA-based TGase 2 assay

As previously shown by Kenniston et al. (Kenniston et al. 2013) and Yamada & Meguro (Yamada and Meguro 1977), transglutaminase-catalyzed cross-linking of small fluorescently labeled peptides and biogenic amines, respectively, to larger proteins results in an increase in fluorescence anisotropy over time and can, thus, be used to quantify the enzyme's activity (Pietsch et al. 2013). The advantages of using FA assays for drug discovery have previously been summarized by Li et al. (Li et al. 2000), who noted that the FA method allows for homogeneous, cost-effective and miniaturizable assays suitable for HTS. In addition, it represents a ratiometric technique and, thus, is "less susceptible to inner-filter interference" (Li et al. 2000). In contrast to assays measuring changes in the fluorescence intensity, FA assays require no change of the fluorophore's properties and show less background noise (Kongsbak et al. 1999).

Despite the fact that the principle behind the reported kinetic TGase FA assays (Yamada and Meguro 1977; Kenniston et al. 2013) appears advantageous, the substrates applied in these studies bear certain drawbacks, such as susceptibility of the protein substrate to transglutaminase-catalyzed crosslinking in addition to defined transamidation between the protein and fluorescent low-molecular weight substrate or employment of a suboptimal fluorophore (dansyl). Therefore, we have chosen DMC as macromolecular acyl donor substrate and three xanthene dye-conjugated cadaverine derivatives (compounds **1**-**3**) as acyl acceptor substrates to establish a FA-based activity assay for TGase 2. While compound **1** [literature-known, e.g. (Lorand et al. 1983)] was labeled with the green fluorescent fluorescein moiety via the reaction with FITC, the two newly developed compounds **2** and **3** contained the orange fluorescent rhodamine B connected to cadaverine by a sarcosyl and an isonipecotyl linker, respectively. Fluorescein-labeled cadaverine is highly effective in cell culture and superior to dansyl cadaverine due to more favorable fluorescence properties and reduced cytotoxicity (Lajemi et al. 1997; Gray et al. 1999; Jameson and Seifried 1999) and has often been used to study TGase 2 activity in living cells (Johnson et al. 1998; Verderio et al. 1998; Gray et al. 1999; Tong et al. 2006; van Geel et al. 2012). The more red-shifted dye rhodamine B has recently been used by Chabot et al. (Chabot et al. 2010) to generate a fluorescent probe for detection of TGase 2 activity in the aorta of rats. This fluorophore was chosen by the authors “due to its hiqh quantum yield and red emission, easily distinguishable from intrinsic cellular fluorescence”.

In accordance with literature (Kenniston et al. 2013), the TGase 2-catalyzed reaction of DMC with cadaverine derivatives **1-3** resulted in a linear increase in FA over time (exemplarily shown for the reaction of DMC with compound **2** in Online Resource Fig. S11). The concentration of the three cadaverine derivatives finally chosen for the assay (0.81 µM) was in a range where interference caused by quenching of fluorescence can be excluded (Online Resource Figs. S10 and S13b). To establish an assay suitable for investigating

inhibition of TGase 2, we had to find a range of linear dependence between the enzyme's activity and concentration under the respective assay conditions, i.e. in the presence of 10 µM DMC (for compounds **1** and **2**) as well as 10 and 30 µM DMC (for compound **3**). As shown in Fig. 2, TGase 2 concentrations of 0.5-5 µg/mL fulfilled this prerequisite, thus, an enzyme concentration of 5 µg/mL was chosen for all further experiments to allow for an optimum measuring range. In addition, the enzyme-catalyzed coupling of compound **3** to DMC was found to be ~4 times faster than that of the other two acyl acceptor substrates, which can be attributed to the larger value V_{max} of the former reaction (see below).

When comparing the sensitivity of our FA-based TGase 2 assay with previously reported methods, the amount of enzyme present in the assay mixture is in the range of TGase 2 concentrations that have often been applied in fluorescence-based approaches with the substrate pairs DMC/dansyl cadaverine and DMC/KXD (Case and Stein 2003; Case et al. 2005; Wu and Tsai 2006; Lai et al. 2008; Schaertl et al. 2010). A similar amount of TGase 2 (7.5 µg/mL) has also been used in a colorimetric assay that follows the hydrolysis of the chromogenic substrate Cbz-Glu(γ-p-nitrophenyl ester)Gly (Pardin et al. 2008; Pardin et al. 2009; Chabot et al. 2010), while methods determining the enzyme's activity by a glutamate dehydrogenase-coupled approach (Case and Stein 2003; Hausch et al. 2003; Choi et al. 2005; Dafik and Khosla 2011; Klöck et al. 2011) need up to ten-fold larger TGase 2 concentrations. Radiometric and ELISA-like approaches belong to the most sensitive methods used for the quantification of the TGase 2 activity. However, these approaches are discontinuous, often time-consuming, and include several steps for quantifying the TGase 2 activity (Jeon et al. 1989; Slaughter et al. 1992; Perez Alea et al. 2009; Schaertl et al. 2010; Pietsch et al. 2013) Although equally sensitive to established fluorescence-based methods using dansyl-labeled substrates, the new assay presented in this study is superior due to the above-mentioned advantages of both kinetic FA measurements and applying cadaverines conjugated with spectro-optically favorable fluorophores as acyl acceptor substrates.

Characterization of the TGase 2-catalyzed reaction of DMC with cadaverine derivatives **1**-**3**

The characterization of the enzyme-substrate interaction was done for the reaction of DMC with each of the cadaverine derivatives **1**-**3**. The results obtained by varying the concentration of DMC in the presence of acyl acceptor substrate at fixed concentration (0.81 µM) are shown in Table 1 and Fig. 3a. The reaction of DMC with FITC cadaverine **1** followed Michaelis-Menten kinetics, while increasing concentrations of DMC led to substrate inhibition (Copeland 2000) with K_i values of 303 µM and 135 µM when the rhodamine B-labeled derivatives **2** and **3** were used as acyl acceptor substrates, respectively. The K_m values determined in the presence of cadaverine derivatives **1** and **2** were in agreement with literature data obtained for the TGase 2-catalyzed reaction of DMC with the acyl acceptor substrate dansyl cadaverine (Case and Stein 2003; Wu and Tsai 2006). This result is supported by Lorand et al. (Lorand et al. 1983) who reported an identical binding behavior of dansyl and FITC cadaverine towards TGase 2 from guinea pig liver.

Interestingly, the combination of DMC and the three cadaverine derivatives **1**-**3** resulted in donor/acceptor pairs with non-significantly different values V_{max}/K_m and, thus, comparable turnover numbers (k_{cat}/K_m). However, when looking separately at K_m and V_{max}, the exchange of the fluorescein-5-aminothiocarbonyl group in **1** for a rhodamine B-sarcosyl moiety in **2** led to a slight increase of the two parameters by factors of 1.7 and 1.4, respectively, while much larger values resulted when the sarcosyl linker in **2** was replaced by an isonipecotyl linker in compound **3** (9.0- and 6.5-fold increase, respectively, compared to **1**). These differences in kinetic behavior might be due to the increasing distance between the cadaverine and xanthenyl moieties from **1** over **2** to **3**. In addition, the lack of rotamerism in **3** potentially contributes to the superiority of **3** over **2**.

When varying the concentration of the acyl acceptor substrates in the presence of a fixed concentration of DMC (~1.1-3.3 × K_m), the cadaverine derivatives **1-3** showed a behavior best described by substrate inhibition (Copeland 2000) (Fig. 3b). This is in accordance with respective data obtained with the acyl acceptor dansyl cadaverine (Case and Stein 2003). Saturation of the enzymatic reactions covered ~2.5 orders of magnitude of the substrate concentration with half-maximal activities in the subnanomolar range (K_m = 0.066-0.24 nM) and substrate inhibition constants in the micromolar range (K_i = 7.1-10 µM). The apparent K_m values of the acyl acceptor substrates determined with the FA assay are, however, far below the reported dissociation constant of FITC cadaverine of 40 µM (Lorand et al. 1983) and several orders of magnitude smaller than the K_m value of dansyl cadaverine (Lorand et al. 1971; Wu and Tsai 2006) and, thus, should not be interpreted kinetically. The observed decline of the velocities at higher concentrations of the xanthene-conjugated cadaverines is probably a reflection of the limit in fluorescence anisotropy. The limitation of the FA values becomes obvious when the transamidation reactions at different concentrations of **1-3** are monitored until completion (Online Resource Fig. S12a): the final FA values increase until ~10 nM of fluorescent substrate and do not further increase at higher concentrations. The complex relationship between fluorescence polarization and fluorophore concentration has been initially observed for solutions of uranin (disodium salt of fluorescein) in glycerin as viscous solvent (Gaviola and Pringsheim 1924). Pheovilov and Sveshnikov (Pheovilov and Sveshnikov 1940) demonstrated that the fluorescence polarization of fluorescein dissolved in glycerin remained virtually constant in a concentration range of 1-100 µM and steeply declined at higher concentrations while the intensity of the fluorescent light is much less affected, which basically matches our observations with the three cadaverine derivatives (Online Resource Fig. S12). This phenomenon is referred to as concentration depolarization and has been interpreted in the light of Förster resonance energy transfer (FRET) [(Förster 1946) see also (Förster 2012) for English translation; (Förster 1948; van der

Meer 2014)]. One fluorophore excited by polarized light may transfer its energy to another fluorophore in close distance via FRET. As an parallel orientation of the light- and FRET-excited fluorophores (an event that would maintain polarization) is unlikely, emission of more depolarized fluorescent light by the FRET-excited fluorophore is highly probable (Valeur 2001). In this context it should be mentioned that measurement of fluorescence anisotropy has been applied as sensitive method to detect FRET in substrates of the botulinum neurotoxin protease. Blue fluorescent protein (BFP) and green fluorescent protein (GFP) have been conjugated to the N- and C-terminus of a fragment derived from the 25 kDa synaptosome-associated protein (SNAP-25). FRET between BFP and GFP results in attenuated polarization of the light emitted from GFP. Proteolytic cleavage suspends FRET and results in an increase in fluorescence polarization despite the molar mass is reduced compared to the quenched substrate (Gilmore et al. 2011; Ross et al. 2011). Concentration depolarization is probably the reason for the observed stagnation of the final FA values with increasing concentration of the fluorescent substrates (Online Resource Fig. S12a). Higher concentrations of casein-bound fluorophores do not result in higher fluorescence anisotropy values probably due to energy transfer between excited fluorophores to ground state fluorophores and therefore a plateau is reached that further decreases at high substrate concentrations. In consequence, the reaction velocities expressed as change in FA per time interval pass through a maximum as observed for the TGase 2-catalyzed conversion of compounds **1**-**3** (Fig. 3b). Notably, the shape of the plots for the final FA values against the substrate concentration resembles those of the velocity plots. Therefore, the observed maxima in the Michaelis-Menten plots of the fluorescent cadaverine derivatives are due to the complex relationship between the concentration of the fluorophore-conjugated casein molecules and fluorescence anisotropy rather than substrate inhibition. These findings are in accordance with results obtained from studies on fluorogenic protease substrates by Frank and Graf (Frank and Graf 1992). In that particular case, non-linearity between the concentration of the fluorescent leaving group and

intensity of fluorescence occurs due to quenching of product fluorescence by unconverted substrate. This phenomenon results in plots of v *versus* [S] that resemble substrate inhibition despite the enzyme actually exhibits Michaelis-Menten behavior.

In consequence to the results discussed above, the concentrations of the fluorescent cadaverine substrates should not exceed 1 µM in order to prevent signal reduction due to quenching (Fig. 3b).

Evaluation of the FA assay for the search and characterization of TGase 2 inhibitors

The new FA-based assay was evaluated towards its potential for the search of TGase 2 ligands by using three established inhibitors of the enzyme, i.e. the two irreversibly interacting compounds iodoacetamide (de Macédo et al. 2000) and compound **4** (Wityak et al. 2012) and the reversible inhibitor GTP (Achyuthan and Greenberg 1987; Mádi et al. 2005; Jang et al. 2014). The inhibitors were investigated after pre-incubation with TGase 2 for 30 min in the presence of the three cadaverine derivatives **1-3** and the results are presented in Table 2 and Figs. 4a, 5, and 6. Dose-dependent saturation was found for all three inhibitors with the activity of TGase 2 being completely abolished at high inhibitor concentrations. Curve fitting was performed considering a variable Hill slope, n_H. However, most of the calculated values n_H were not significantly different from one and did not depend on the acyl acceptor substrate used (Table 2).

Iodoacetamide and compound **4** inhibited TGase 2 with IC_{50} values of about 0.02 µM and 0.27 µM, with the values obtained in the presence of the three cadaverine derivatives **1-3** being not significantly different. The IC_{50} value of iodacetamide is similar to half the amount of active enzyme used in these experiments ($[E]_{active}$ = 52.6 nM, calculated on the basis of data provided by the vendor), proving that iodoacetamide completely inactivates TGase 2 within the pre-incubation time (30 min). This is not the case for compound **4**, which exhibits

an IC_{50} value that is one order of magnitude higher than both that of iodoacetamide as well as that obtained by Wityak et al. (Wityak et al. 2012) for **4** on human TGase 2 (14 nM), with the difference to the latter value might being attributed to the different source (guinea pig *versus* human) and amount of enzyme. In addition, as shown to some extent in this study, any difference in the experimental setup, such as buffer conditions, pre-incubation time (particularly important for irreversible inhibitors), enzyme amount and both type and concentration of the substrates, strongly influences the IC_{50} value, which, thus, should rather be used for comparing data of the same study than for comparison of results with literature values (Copeland 2005; Shoichet 2006; Krippendorff et al. 2009; Stein 2011).

Inhibition of TGase 2 by GTP was initially investigated with DMC (10 µM) and cadaverine derivative **1** (0.81 µM) at pH 8.0 (MOPS buffer) as done for iodoacetamide and compound **4** (Online Resource Fig. S13a). Due to the known dependency of the IC_{50} of GTP on the Ca^{2+} concentration (Achyuthan and Greenberg 1987; Case et al. 2005), experiments were, however, performed in the presence of 1 mM $CaCl_2$ resulting in an IC_{50} of 691 µM. Lowering the pH to 7.4 (HEPES buffer) (Case et al. 2005) led to a decrease of the inhibition constant to 67 µM (Table 2, Fig. 6), which is in the range of the reported K_i value of 90 µM (Achyuthan and Greenberg 1987). Therefore, the latter buffer system was used for all experiments including GTP. Exchanging FITC cadaverine **1** for the rhodamine B derivatives **2** and **3** resulted in an (significant) increase of IC_{50} to 91 µM and 109 µM, respectively (Table 2). The inhibition constant in the presence of acyl acceptor **3** was obtained with 10 µM DMC instead of 30 µM DMC (applied in the characterization of iodoacetamide and compound **4**) as the higher concentration of DMC caused a three-fold increase of IC_{50} (Online Resource Fig. S13b). This behavior is in line with the observation that GTP and other guanine nucleotides act as potent allosteric inhibitors by binding to the closed transglutaminase-inactive conformation of TGase 2 (Liu et al. 2002; Jang et al. 2014), whereas interaction of the enzyme with the acyl donor substrate or inhibitors derived thereof stabilizes the open

transglutaminase-active conformation of TGase 2 (Gross and Folk 1973; Pinkas et al. 2007). As a result, increasing the concentration of DMC seems to counteract the inhibition of TGase 2 by allosteric GTP-like compounds and, thus, DMC concentrations greater than applied in this study might hamper the identification of inhibitors of this type. So far, data obtained on the mode of inhibition of GTP and its non-hydrolysable derivative guanosine 5′-[β,γ-imido]triphosphate (GMP-PNP) remain, however, controversial. While Piper et al. (Piper et al. 2002) found a competitive mode of inhibition, which might be explained by the contrary effects of substrate and inhibitor on the conformation of TGase 2, Achyuthan and Greenberg (Achyuthan and Greenberg 1987) described GTP as a non-competitive inhibitor. The latter mode of inhibition is supported by Lai et al. (Lai et al. 1998) who reported a similar inhibition constant for GTP when the substrate concentration was lowered 25-fold.

Active-site titration of TGase 2

Titration of the active-site cysteine was done by alkylation with iodoacetamide, which is known to be able to alkylate TGase 2 in an equimolar manner (Folk and Cole 1966a, b). However, while several groups have reported a direct approach for the determination of the active concentration of TGases using ^{14}C-labeled iodacetamide (Folk and Cole 1966a; Chang and Chung 1986; Kim et al. 1994; Rossi et al. 2000), we applied an indirect method by measuring the inhibition of the TGase 2-catalyzed reaction between DMC and cadaverine derivatives **1**-**3** by iodoacetamide (Fig. 7, Online Resource Fig. S14). For this purpose, we were able to use the data obtained during the evaluation of the inhibitor in the FA assay (Fig. 4a), yielding active TGase 2 concentrations of 43.9 ± 5.6 nM, 47.0 ± 2.7 nM and 47.9 ± 8.5 nM (Mean ± SD) when compounds **1**, **2** and **3** were used as acyl acceptor substrate, respectively. The results obtained in the presence of the three cadaverine derivatives are not significantly different from each other (one-way ANOVA with Tukey's multiple comparison

test, $P > 0.05$) and correspond to 67.3 ± 8.6%, 72.0 ± 4.2%, and 73.4 ± 13.0% of the protein concentration applied in the assay, respectively, with these three percentages being not significantly different from the content of active TGase 2 (80.6%) calculated on the basis of information provided by the vendor (Zedira, Darmstadt, Germany). The applied method is fast, simple, and does not require the separation of labeled protein from the reaction mixture, which is usually necessary in the case of active-site titrations with radioactive compounds (Folk and Cole 1966a; Kim et al. 1994; Rossi et al. 2000). Folk and colleagues (Folk et al. 1967; Folk and Gross 1971; Folk 1982) have reported both direct and indirect non-radioactive approaches to obtain the active TGase 2 concentration by spectrophotometric titration using the inhibitors α-bromo-4-hydroxy-3-nitroacetophenone (BHNA) and methyl *N*-(2-hydroxy-5-nitrophenylacetyl)-L-2-amino-4-oxo-5-chloropentanoate (L-PACK), and the substrate nitrophenyl pivalate. However, while these methods use TGase 2 concentrations in the two-digit micromolar range, our FA assay is circa three orders of magnitude more sensitive.

Z' factor of the FA-based TGase 2 assay

The suitability of the FA assay for HTS was investigated by determination of the Z' factor according to Zhang et al. (Zhang et al. 1999), which serves as a measure for overall assay quality and "reproducibility of hit identification". For this purpose, we analyzed the TGase 2-catalyzed reaction of DMC (30 µM) and compound **3** (0.81 µM), which exhibited the most favorable substrate properties of the three cadaverine derivatives studied, according to Kenniston et al. (Kenniston et al. 2013) (Fig. 4b). In the negative control, 10 µM iodoacetamide were present in the assay mixture to ensure complete inhibition of TGase 2 (5 µg/mL), while the positive control contained the same amount enzyme in the absence of inhibitor. The guinea pig liver TGase 2 used in these experiments was recombinantly produced in *E. coli* and behaved identical to the isolated enzyme (Online Resource Fig. S15)

that was applied in the validation of the inhibitors iodoacetamide, compound **4**, and GTP. Calculation of the Z' factor gave an excellent value of 0.86 (Zhang et al. 1999), with the same value being obtained when the calculation based on the anisotropy values taken from the end of the kinetic run (after 15 min, Online Resource Fig. S16). This value is in the range of Z' factors (0.7-0.9) commonly found for HTS-enabled FA assays (Jameson and Ross 2010; Kenniston et al. 2013) and TGase 2 assays with fluorometric, radiometric or colorimetric readouts (Case et al. 2005; Mádi et al. 2005; Perez Alea et al. 2009) and, thus, proves the high suitability of both the kinetic FA assay and the respective endpoint assay for the search of TGase 2 inhibitors.

Conclusion

In conclusion, we present a kinetic method to assay TGase 2, which follows the time-dependent increase in fluorescence anisotropy due to the enzyme-catalyzed transamidation between DMC and the three efficiently synthesized fluorescein-/rhodamine B-conjugated cadaverine derivatives **1**-**3**. Advantages of the new assay are the homogeneous design, the excellent reproducibility, and the lack of background signal in the absence of TGase 2. Due to its superior substrate properties (in particular the high V_{max}), the rhodamine B-conjugated acyl acceptor **3** was identified as very suitable for HTS of both reversible and irreversible TGase 2 inhibitors. By characterizing the established inhibitor iodoacetamide with the new assay, we found a simple and sensitive method for active-site titration of TGase 2, circumventing the problems of known radioactive and spectrophotometric approaches. In addition, the potent rhodamine B-labeled cadaverine derivative **3** bears the potential to be used as tool for characterizing TGase 2's transamidation activity at a cellular level as well as in tissues and living organisms due to its favorable kinetic and spectral properties.

Although the presented FA assay exhibits many advantages for the characterization of the in vitro activity and inhibition of isolated TGase 2, the acyl donor substrate DMC – abundantly employed in the screening and development of TGase 2 inhibitors (Pietsch et al. 2013) – was previously shown to lack specificity for TGase 2. Other members of the TGase family, such as factor XIIIa and TGases 1, 3, 6, and 7, exhibit comparable activities when assayed with DMC/dansyl cadaverine or DMC/KXD (Schaertl et al. 2010; Yamane et al. 2010; Prime et al. 2012; Kuramoto et al. 2013). These findings leave to conclude that the application of such substrate pairs will not allow studying single TGase isozymes or discriminating TGases in complex mixtures. To circumvent this dilemma, isozyme-selective, low-molecular weight inhibitors, such as compound **4** (Wityak et al. 2012), might be used for

studying TGase 2 in cell lysates and tissue homogenates with the FA-based assay established herein, which is under current investigation in our laboratories.

Tables

Table 1 Kinetic parameters of the substrate DMC for its TGase 2-catalyzed reaction with cadaverines[a]

	1	**2**	**3**
	$n = 3$	$n = 4$	$n = 3$
K_m (µM)	3.05 ± 0.44	5.06 ± 0.74	27.5 ± 6.4
K_i (µM)	-	303 ± 45	135 ± 32
V_{max} (mA s^{-1})	0.0270 ± 0.0021	0.0379 ± 0.0020	0.176 ± 0.028
V_{max}/K_m (mA s^{-1} μM^{-1})[b]	0.00948 ± 0.00215	0.00783 ± 0.00080	0.00665 ± 0.00067

[a] Mean values ± SEM of *n* experiments

[b] Values V_{max}/K_m obtained for DMC with cadaverine derivatives **1**, **2** and **3** were subjected to a one-way ANOVA with Tukey's multiple comparison test. No significant difference was found ($P > 0.05$)

Table 2 Inhibition parameters IC_{50} and n_H of reference TGase 2 inhibitors[a]

	1	**2**	**3**
Iodoacetamide	*n* = 3	*n* = 3	*n* = 3
IC_{50} (µM)[b]	0.0187 ± 0.0019	0.0217 ± 0.0020	0.0207 ± 0.0039
n_H[b]	-1.62 ± 0.14[c]	-1.57 ± 0.15	-1.54 ± 0.16
4	*n* = 4	*n* = 3	*n* = 3
IC_{50} (µM)[b]	0.271 ± 0.035	0.267 ± 0.009	0.277 ± 0.006
n_H[b]	-1.45 ± 0.15	-1.15 ± 0.04	-1.36 ± 0.05[c]
GTP	*n* = 4	*n* = 3	*n* = 3
IC_{50} (µM)[b]	66.6 ± 7.2	91.4 ± 10.9	109 ± 7[*]
n_H[b]	-0.771 ± 0.030[c]	-0.838 ± 0.052	-0.847 ± 0.039

[a] Mean values ± SEM of *n* experiments

[b] Values IC_{50} and n_H obtained for the inhibitor with cadaverine derivatives **1**, **2** and **3** were subjected to a one-way ANOVA with Tukey's multiple comparison test. No significant difference was found ($P > 0.05$) if not stated otherwise. [*], $P \leq 0.05$ for the IC_{50} values obtained with **1** and **3**

[c] All values n_H were subjected to a One-sample t-test, with those values labeled with "[c]" being significantly different from $n_H = -1$ ($P \leq 0.05$)

Schemes

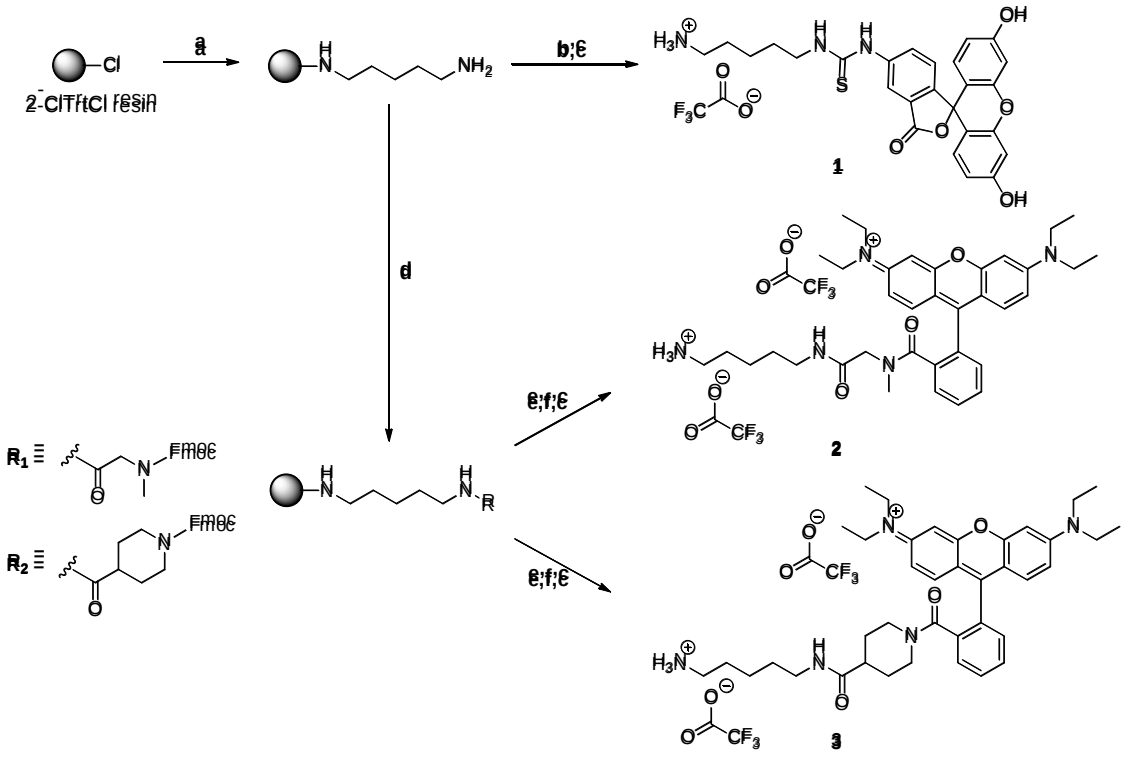

Scheme 1 Synthesis of the cadaverine derivatives **1**-**3** (**1**, MW = 605.58 g/mol; **2**, MW = 825.84 g/mol; **3**, MW = 865.90 g/mol). Reagents and conditions: a) 1. cadaverine, CH_2Cl_2, 17 h; 2. CH_2Cl_2/CH_3OH/DIPEA (17/1/2). b) fluorescein-5-isothiocyanate, TEA, DMF, 8h. c) TFA/TES/H_2O (95:2.5:2.5), 2 h. d) 1. Fmoc-Sar-OH or Fmoc-Inp-OH, PyBOP, DIPEA, DMF, 5 h; 2. 0.5 M acetic anhydride/DIPEA in DMF. e) 20% piperidine/DMF. f) rhodamine B, HATU, DIPEA, DMF, 5 h. All reactions were carried out at ambient temperature

Legends to Figures

Fig. 1 Structures of the TGase 2 inhibitors used in this study: L-lysine acrylamide derivative **4**, iodoacetamide, and GTP

Fig. 2 Plots of the rate versus the gpTGase 2 concentration for the reaction of DMC (**1**, **2**: 10 µM; **3**: 30 µM) with **1** (0.81 µM, black open symbols), **2** (0.81 µM, grey filled symbols), and **3** (0.81 µM, black filled symbols), respectively. Data shown are mean values ± SEM of 3-4 separate experiments, each performed in triplicate. Analysis by linear regression gave slopes (mean values ± SEM) of 0.00424 ± 0.00020 mA mL s^{-1} μg^{-1} (**1**, n = 4), 0.00488 ± 0.00017 mA mL s^{-1} μg^{-1} (**2**, n = 3), and 0.0187 ± 0.0031 mA mL s^{-1} μg^{-1} (**3**, n = 3). The gpTGase 2-catalyzed reaction of DMC (10 µM) with **3** (0.81 µM) gave a linear dependency of the enzyme's activity on the concentration (data not shown) with a slope of 0.0179 ± 0.0006 mA mL s^{-1} μg^{-1} (n = 3), that is not significantly different from the result obtained with 30 µM DMC (unpaired two sample Student's t test, $P > 0.05$)

Fig. 3 a) Plots of the rate versus the substrate concentration for the reaction of DMC with **1** (0.81 µM, black open symbols), **2** (0.81 µM, grey filled symbols), and **3** (0.81 µM, black filled symbols) respectively, in the presence (circles) and absence (squares) of gpTGase 2 (5 µg/mL). Data shown are mean values ± SEM of 2-4 separate experiments, each performed in triplicate The reactions in the presence of gpTGase 2 followed standard Michaelis-Menten behavior (**1**) or that of substrate inhibition (**2**, **3**) (Copeland 2000). Results are shown in Table 1. b) Plots of the rate versus substrate concentration for the reaction of DMC (**1**, **2**: 5 µM; **3**: 30 µM) with **1** (black open symbols), **2** (grey filled symbols), and **3** (black filled symbols), respectively, in the presence (circles) and absence (squares) of gpTGase 2 (5 µg/mL). Data shown are mean values ± SEM of 3 separate experiments, each performed in triplicate. The

reactions in the presence of enzyme were analyzed according to the equation of substrate inhibition (Copeland 2000) (mean values ± SEM, n = 3): **1**, K_m = 0.222 ± 0.140 nM, K_i = 9.15 ± 3.11 µM, and V_{max} = 0.0181 ± 0.0005 mA s^{-1}; **2**, K_m = 0.0661 ± 0.0367 nM, K_i = 10.2 ± 2.0 µM, and V_{max} = 0.0181 ± 0.0011 mA s^{-1}; **3**, K_m = 0.242 ± 0.069 nM, K_i = 7.14 ± 2.20 µM, and V_{max} = 0.113 ± 0.013 mA s^{-1}

Fig. 4 a) Inhibition of gpTGase 2 (5 µg/mL) by iodoacetamide determined with the substrates DMC (**1**, **2**: 10 µM; **3**: 30 µM) and **1** (0.81 µM, black open symbols), **2** (0.81 µM, grey filled symbols), and **3** (0.81 µM, black filled symbols), respectively. Data shown for the reaction in the presence (circles) and absence (squares) of enzyme are mean values ± SEM of 2-3 separate experiments, each performed in triplicate. Results are shown in Table 2. b) Determination of the Z' factor for the reaction of DMC (30 µM) with cadaverine derivative **3** (0.81 µM) catalyzed by recombinant guinea pig liver TGase 2 (5 µg/mL) in the absence (circles) and presence (squares) of iodoacetamide (10 µM). Rates obtained in three separate experiments are shown, with 23-24 wells being used for each of the two conditions per experiment. A Z' factor of 0.861 ± 0.011 (mean ± SEM, n = 3) was calculated by applying the equation $Z' = 1 - [(3SDrate_{free} + 3SDrate_{inhibited})/(|meanrate_{free} - meanrate_{inhibited}|)]$ to each experiment, where SD and mean are the standard deviations and mean values of the rates, respectively, of those wells containing either the free gpTGase 2 or the fully inhibited enzyme (Zhang et al. 1999)

Fig. 5 Inhibition of gpTGase 2 (5 µg/mL) by compound **4** determined with the substrates DMC (**1**, **2**: 10 µM; **3**: 30 µM) and **1** (0.81 µM, black open symbols), **2** (0.81 µM, grey filled symbols), and **3** (0.81 µM, black filled symbols), respectively. Data shown for the reaction in

the presence (circles) and absence (squares) of enzyme are mean values ± SEM of 3-4 separate experiments, each performed in duplicate or triplicate. Results are shown in Table 2

Fig. 6 Inhibition of gpTGase 2 (5 µg/mL) by GTP determined with the substrates DMC (10 µM) and **1** (0.81 µM, black open symbols), **2** (0.81 µM, grey filled symbols), and **3** (0.81 µM, black filled symbols), respectively. Data shown for the reaction in the presence (circles) and absence (squares) of enzyme are mean values ± SEM of 3-4 separate experiments, each performed in a single measurement, in duplicate, or triplicate. Results are shown in Table 2

Fig. 7 Active site titration of gpTGase 2 (5 µg/mL) using the inhibitor iodacetamide and the substrates DMC (30 µM) and compound **3** (0.81 µM). Data shown for the reaction in the presence of enzyme are taken from Fig. 4a and represent mean values ± SEM of 3 separate experiments, each performed in triplicate. A theoretical total enzyme concentration, E_{tot}, was calculated to 65.3 nM (M_r = 76.6 kDa, information provided by Zedira, Darmstadt, Germany) assuming all protein to be gpTGase 2. Data obtained with inhibitor concentrations below E_{tot} (circles) and above E_{tot} (triangles) were separately subjected to linear regression.The x-value of the intersection point of the lines, that corresponds to the active enzyme concentration, was calculated with the equation $x = (n_2-n_1)/(m_1-m_2)$, with m and n representing the slopes and the intercepts of the two lines, respectively. An active enzyme concentration of 47.9 ± 8.5 nM (Mean ± SD), i.e. 73.4 ± 13.0% active gpTGase 2 with regards to the total protein concentration, was calculated, which is not significantly different (One-sample t-test, $P > 0.05$) from the content of active enzyme (80.6%) calculated on the basis of activity data (hydroxamate assay) (Folk and Cole 1966c) provided by the vendor

Figures

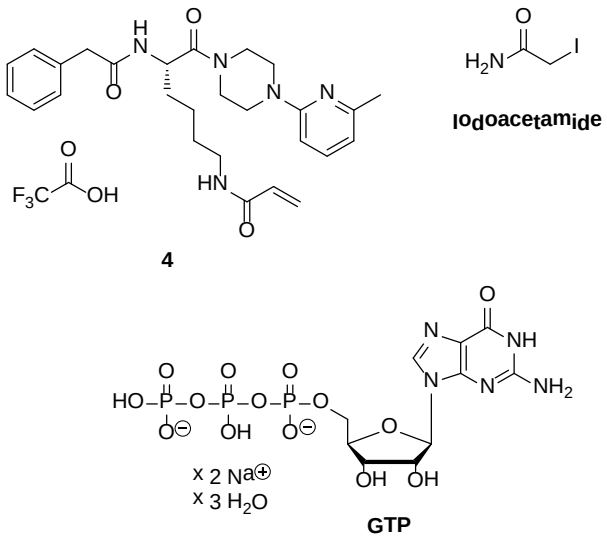

Fig. 1

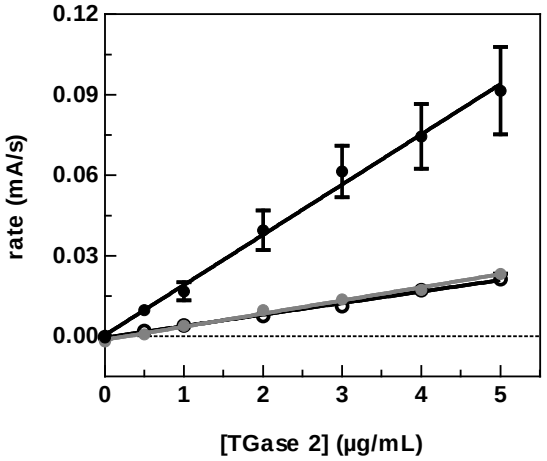

Fig. 2

a)

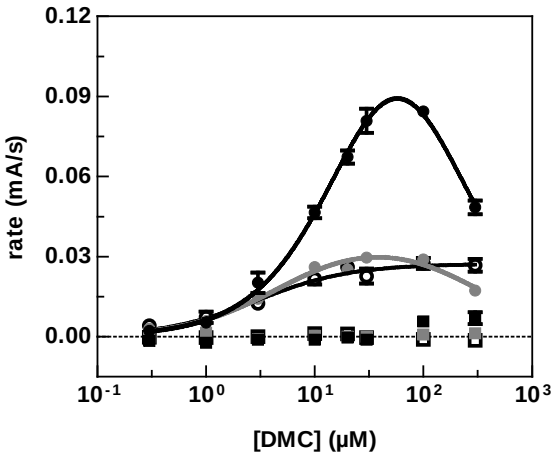
0.12
0.09
0.06
0.03
0.00
rate (mA/s)
10-1
100
101
102
103
[DMC] (μM)

b)

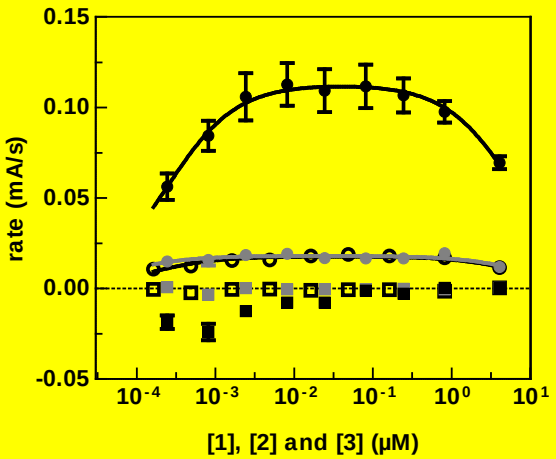
0.15
0.10
0.05
0.00
-0.05
rate (mA/s)
10-4
10-3
10-2
10-1
100
101
[1], [2] and [3] (μM)

Fig. 3

a)

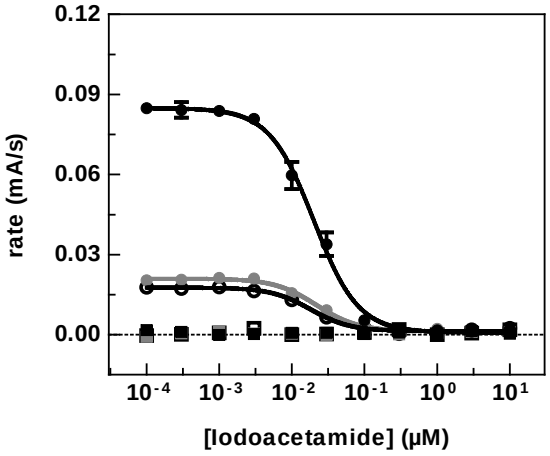
0.12
0.09
0.06
0.03
0.00
rate (mA/s)
10-4
10-3
10-2
10-1
100
101
[Iodoacetamide] (µM)

b)

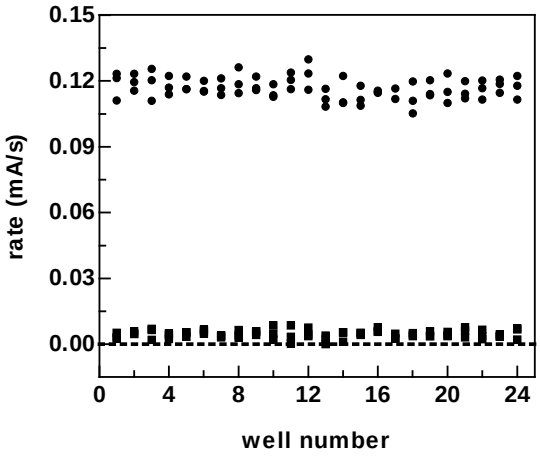
0.15
0.12
0.09
0.06
0.03
0.00
rate (mA/s)
0
4
8
12
16
20
24
well number

Fig. 4

a)

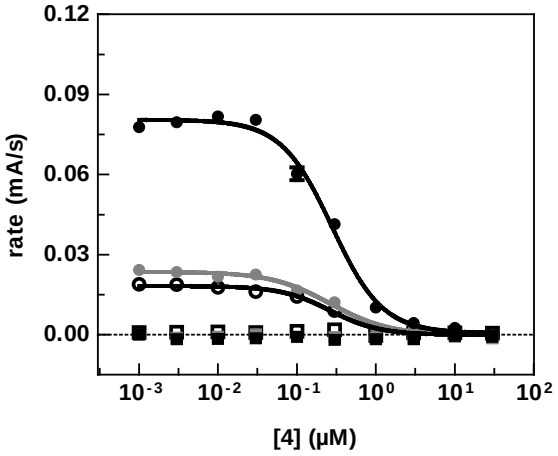

Fig. 5

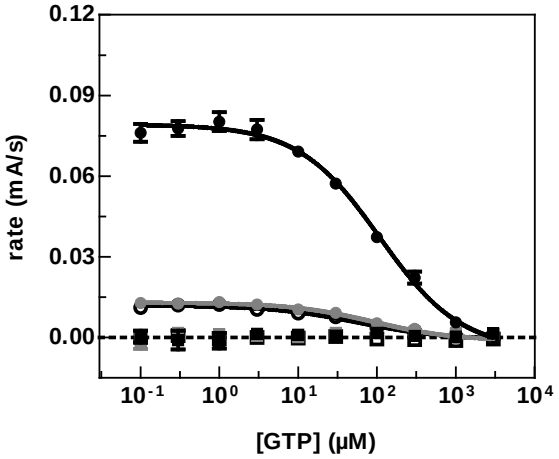

Fig. 6

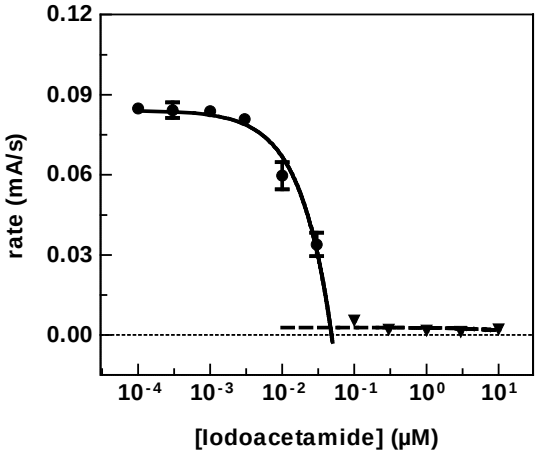
0.12
0.09
0.06
0.03
0.00
rate (mA/s)
10-4
10-3
10-2
10-1
100
101
[Iodoacetamide] (µM)

Fig. 7

Acknowledgements

The authors thank Martin Lohse (Helmholtz-Zentrum Dresden-Rossendorf, Institute of Radiopharmaceutical Cancer Research) for assisting in the synthesis of compound **3**.
C. H. and M. P. are grateful for support to the Graduate Program in Pharmacology and Experimental Therapeutics of the University of Cologne and the Bayer Health Care AG (Project No. O23). C. H. acknowledges financial support by the Friedrich-Naumann-Stiftung für die Freiheit (ST 6479/ P 622). Partial financial support by the Helmholtz Portfolio Topic "Technologie und Medizin – Multimodale Bildgebung zur Aufklärung des in vivo-Verhaltens von polymeren Biomaterialien" (R. W. and R. L.) and by the Fonds der Chemischen Industrie (R. L.) is gratefully acknowledged.

Conflict of interest

Funding by the Bayer Health Care AG to C. H. and M. P. has been received via the University of Cologne without any economic obligation. R. W. and R. L. declare that they have no conflict of interest.

Research involving human participants and/or animals; Informed consent

This article does not contain any studies with human participants or animals performed by any of the authors. Obtaining informed consent was, therefore, not necessary.

References

Achyuthan KE, Greenberg CS (1987) Identification of a guanosine triphosphate-binding site on guinea-pig liver transglutaminase - role of GTP and calcium-ions in modulating activity. J Biol Chem 262 (4):1901-1906

Adamczyk M, Grote J (2000) Efficient synthesis of rhodamine conjugates through the 2'-position. Bioorg Med Chem Lett 10 (14):1539-1541

Agnihotri N, Kumar S, Mehta K (2013) Tissue transglutaminase as a central mediator in inflammation-induced progression of breast cancer. Breast Cancer Res 15 (1):202

Anthoni U, Christophersen C, Nielsen PH, Puschl A, Schaumburg K (1995) Structure of red and orange fluorescein. Struct Chem 6 (3):161-165

Badarau E, Collighan RJ, Griffin M (2013) Recent advances in the development of tissue transglutaminase (TG2) inhibitors. Amino Acids 44 (1):119-127

Beija M, Afonso CAM, Martinho JMG (2009) Synthesis and applications of rhodamine derivatives as fluorescent probes. Chem Soc Rev 38 (8):2410-2433

Beninati S, Facchiano F, Piacentini M (2013) Transglutaminases: future perspectives. Amino Acids 44 (1):1-9

Bernecker A, Wieneke R, Riedel R, Seibt M, Geyer A, Steinem C (2010) Tailored synthetic polyamines for controlled biomimetic silica formation. J Am Chem Soc 132 (3):1023-1031

Blommel PG, Fox BG (2005) Fluorescence anisotropy assay for proteolysis of specifically labeled fusion proteins. Anal Biochem 336 (1):75-86

Brauch S, Henze M, Osswald B, Naumann K, Wessjohann LA, van Berkel SS, Westermann B (2012) Fast and efficient MCR-based synthesis of clickable rhodamine tags for protein profiling. Org Biomol Chem 10 (5):958-965

Case A, Ni J, Yeh LA, Stein RL (2005) Development of a mechanism-based assay for tissue transglutaminase--results of a high-throughput screen and discovery of inhibitors. Anal Biochem 338 (2):237-244

Case A, Stein RL (2003) Kinetic analysis of the action of tissue transglutaminase on peptide and protein substrates. Biochemistry 42 (31):9466-9481

Case A, Stein RL (2007) Kinetic analysis of the interaction of tissue transglutaminase with a nonpeptidic slow-binding inhibitor. Biochemistry 46 (4):1106-1115

Chabot N, Moreau S, Mulani A, Moreau P, Keillor JW (2010) Fluorescent probes of tissue transglutaminase reveal its association with arterial stiffening. Chem Biol 17 (10):1143-1150

Chang SK, Chung SI (1986) Cellular transglutaminase. The particulate-associated transglutaminase from chondrosarcoma and liver: partial purification and characterization. J Biol Chem 261 (18):8112-8121

Choi K, Siegel M, Piper JL, Yuan L, Cho E, Strnad P, Omary B, Rich KM, Khosla C (2005) Chemistry and biology of dihydroisoxazole derivatives: Selective inhibitors of human transglutaminase 2. Chem Biol 12 (4):469-475

Cleemann F, Karuso P (2008) Fluorescence anisotropy assay for the traceless kinetic analysis of protein digestion. Anal Chem 80 (11):4170-4174

Cobas C, Dominguez S, Larin N, Iglesias I, Geada C, Seoane F, Sordo M, Monje P, Fraga S, Cobas R, Peng C, Garcia JA, Goebel M, Vaz E (2010) MestReNova 6.1.1-6384. Mestrelab Research S.L., Bajo, Santiago de Compostela, Spain

Copeland RA (2000) Enzymes: A practical introduction to structure, mechanism, and data analysis. 2nd edn. Wiley-VCH, New York, pp 109-145

Copeland RA (2005) Evaluation of enzyme inhibitors in drug discovery : a guide for medicinal chemists and pharmacologists. Methods of biochemical analysis, vol 46. Wiley-Interscience, Hoboken, N.J., pp 72, 115-117

Dafik L, Khosla C (2011) Dihydroisoxazole Analogs for Labeling and Visualization of Catalytically Active Transglutaminase 2. Chem Biol 18 (1):58-66

de Macédo P, Marrano C, Keillor JW (2000) A direct continuous spectrophotometric assay for transglutaminase activity. Anal Biochem 285 (1):16-20

Egner BJ, Cardno M, Bradley M (1995) Linkers for combinatorial chemistry and reaction analysis using solid phase in situ mass spectrometry. J Chem Soc Chem Commun (21):2163-2164

Folk JE (1982) The trimethylacetyl transglutaminase complex. Method Enzymol 87:36-42

Folk JE, Cole PW (1966a) Identification of a functional cysteine essential for the activity of guinea pig liver transglutaminase. J Biol Chem 241 (13):3238-3240

Folk JE, Cole PW (1966b) Mechanism of action of guinea pig liver transglutaminase. I. Purification and properties of enzyme - identification of a functional cysteine essential for activity. J Biol Chem 241 (23):5518-5525

Folk JE, Cole PW (1966c) Transglutaminase: mechanistic features of the active site as determined by kinetic and inhibitor studies. Biochim Biophys Acta 122 (2):244-264

Folk JE, Cole PW, Mullooly JP (1967) Mechanism of action of guinea pig liver transglutaminase. IV. The trimethylacyl enzyme. J Biol Chem 242 (19):4329-4333

Folk JE, Gross M (1971) Mechanism of action of guinea pig liver transglutaminase. VIII. Active site studies with "reporter" group-labeled halomethyl ketones. J Biol Chem 246 (21):6683-6691

Förster T (1946) Energiewanderung und Fluoreszenz. Naturwissenschaften 33 (6):166-175

Förster T (1948) Zwischenmolekulare Energiewanderung und Fluoreszenz. Ann Phys (Berlin) 2 (1-2):55-75

Förster T (2012) Energy migration and fluorescence. J Biomed Opt 17 (1):011002

Frank HG, Graf R (1992) Interference of substrate quenching with the kinetics of placental peptidases. Biol Chem Hoppe Seyler 373 (10):1031-1038

Fürniss D, Mack T, Hahn F, Vollrath SB, Koroniak K, Schepers U, Bräse S (2013) Peptoids and polyamines going sweet: Modular synthesis of glycosylated peptoids and polyamines using click chemistry. Beilstein J Org Chem 9:56-63

Gaviola E, Pringsheim P (1924) Über den Einfluß der Konzentration auf die Polarisation der Fluoreszenz von Farbstofflösungen. Z Phys 24 (1):24-36

Gilmore MA, Williams D, Okawa Y, Holguin B, James NG, Ross JA, Aoki KR, Jameson DM, Steward LE (2011) Depolarization after resonance energy transfer (DARET): a sensitive fluorescence-based assay for botulinum neurotoxin protease activity. Anal Biochem 413 (1):36-42

Gomes J, Huber N, Grunau A, Eberl L, Gademann K (2013) Fluorescent labeling agents for quorum-sensing receptors (FLAQS) in live cells. Chem Eur J 19 (30):9766-9770

Gray AC, Garle MJ, Clothier RH (1999) Fluorescein cadaverine incorporation as a novel technique for the characterization of terminal differentiation in keratinocytes. Toxicol in Vitro 13 (4-5):773-778

Grimm JB, Heckman LM, Lavis LD (2013) The chemistry of small-molecule fluorogenic probes. Prog Mol Biol Transl Sci 113:1-34

Gross M, Folk JE (1973) Mapping of the active sites of transglutaminases. I. Activity of the guinea pig liver enzyme toward aliphatic amides. J Biol Chem 248 (4):1301-1306

Hausch F, Halttunen T, Maki M, Khosla C (2003) Design, synthesis, and evaluation of gluten peptide analogs as selective inhibitors of human tissue transglutaminase. Chem Biol 10 (3):225-231

Ientile R, Curro M, Caccamo D (2015) Transglutaminase 2 and neuroinflammation. Amino Acids 47 (1):19-26

Jameson DM, Ross JA (2010) Fluorescence polarization/anisotropy in diagnostics and imaging. Chem Rev 110 (5):2685-2708

Jameson DM, Seifried SE (1999) Quantification of protein-protein interactions using fluorescence polarization. Methods 19 (2):222-233

Jang TH, Lee DS, Choi K, Jeong EM, Kim IG, Kim YW, Chun JN, Jeon JH, Park HH (2014) Crystal structure of transglutaminase 2 with GTP complex and amino acid sequence evidence of evolution of GTP binding site. Plos One 9 (9):e107005

Jeon WM, Lee KN, Birckbichler PJ, Conway E, Patterson MK (1989) Colorimetric assay for cellular transglutaminase. Anal Biochem 182 (1):170-175

Jeong JM, Murthy SN, Radek JT, Lorand L (1995) The fibronectin-binding domain of transglutaminase. J Biol Chem 270 (10):5654-5658

Johnson TS, Scholfield CI, Parry J, Griffin M (1998) Induction of tissue transglutaminase by dexamethasone: its correlation to receptor number and transglutaminase-mediated cell death in a series of malignant hamster fibrosarcomas. Biochem J 331 (1):105-112

Kanchan K, Fuxreiter M, Fésüs L (2015) Physiological, pathological, and structural implications of non-enzymatic protein–protein interactions of the multifunctional human transglutaminase 2. Cell Mol Life Sci 72 (16):3009-3035

Keillor JW, Apperley KY, Akbar A (2015) Inhibitors of tissue transglutaminase. Trends Pharmacol Sci 36 (1):32-40

Keillor JW, Clouthier CM, Apperley KYP, Akbar A, Mulani A (2014) Acyl transfer mechanisms of tissue transglutaminase. Bioorg Chem 57:186-197

Kenniston JA, Conley GP, Sexton DJ, Nixon AE (2013) A homogeneous fluorescence anisotropy assay for measuring transglutaminase 2 activity. Anal Biochem 436 (1):13-15

Kim SY, Kim IG, Chung SI, Steinert PM (1994) The structure of the transglutaminase 1 enzyme. Deletion cloning reveals domains that regulate its specific activity and substrate specificity. J Biol Chem 269 (45):27979-27986

Klöck C, Jin X, Choi KH, Khosla C, Madrid PB, Spencer A, Raimundo BC, Boardman P, Lanza G, Griffin JH (2011) Acylideneoxoindoles: A new class of reversible inhibitors of human transglutaminase 2. Bioorg Med Chem Lett 21 (9):2692-2696

Kolmakov K, Wurm CA, Hennig R, Rapp E, Jakobs S, Belov VN, Hell SW (2012) Red-emitting rhodamines with hydroxylated, sulfonated, and phosphorylated dye residues and their use in fluorescence nanoscopy. Chem-Eur J 18 (41):12986-12998

Kongsbak L, Jorgensen KS, Valbjorn J, Jorgensen CT, Husum TL, Ernst S, Moller S (1999) A fluorescence polarization screening method. Denmark Patent WO9945143 (A2), 19990910

Krippendorff B, Neuhaus R, Lienau P, Reichel A, Huisinga W (2009) Mechanism-based inhibition: deriving K_I and k_{inact} directly from time-dependent IC_{50} values. J Biomol Screen 14 (8):913-923

Kuramoto K, Yamasaki R, Shimizu Y, Tatsukawa H, Hitomi K (2013) Phage-displayed peptide library screening for preferred human substrate peptide sequences for transglutaminase 7. Arch Biochem Biophys 537 (1):138-143

Lai TS, Liu Y, Tucker T, Daniel KR, Sane DC, Toone E, Burke JR, Strittmatter WJ, Greenberg CS (2008) Identification of chemical inhibitors to human tissue transglutaminase by screening existing drug libraries. Chem Biol 15 (9):969-978

Lai TS, Slaughter TF, Peoples KA, Hettasch JM, Greenberg CS (1998) Regulation of human tissue transglutaminase function by magnesium-nucleotide complexes. Identification of distinct binding sites for Mg-GTP and Mg-ATP. J Biol Chem 273 (3):1776-1781

Lajemi M, Demignot S, Borge L, Thenet-Gauci S, Adolphe M (1997) The use of fluoresceincadaverine for detecting amine acceptor protein substrates accessible to active transglutaminase in living cells. Histochem J 29 (8):593-606

Lavis LD, Raines RT (2014) Bright building blocks for chemical biology. ACS Chem Biol 9 (4):855-866

Lea WA, Simeonov A (2011) Fluorescence polarization assays in small molecule screening. Expert Opin Drug Discov 6 (1):17-32

Lentini A, Abbruzzese A, Provenzano B, Tabolacci C, Beninati S (2013) Transglutaminases: key regulators of cancer metastasis. Amino Acids 44 (1):25-32

Li Z, Mehdi S, Patel I, Kawooya J, Judkins M, Zhang W, Diener K, Lozada A, Dunnington D (2000) An ultra-high throughput screening approach for an adenine transferase using fluorescence polarization. J Biomol Screen 5 (1):31-38

Liu S, Cerione RA, Clardy J (2002) Structural basis for the guanine nucleotide-binding activity of tissue transglutaminase and its regulation of transamidation activity. Proc Natl Acad Sci U S A 99 (5):2743-2747

Lorand L, Lockridge OM, Campbell LK, Myhrman R, Bruner-Lorand J (1971) Transamidating enzymes. II. Continuous fluorescent method suited for automating measurements of factor XIII in plasma. Anal Biochem 44 (1):221-231

Lorand L, Parameswaran KN, Velasco PT, Hsu LKH, Siefring GE (1983) New colored and fluorescent amine substrates for activated fibrin stabilizing factor (factor $XIII_a$) and for transglutaminase. Anal Biochem 131 (2):419-425

Mádi A, Kárpáti L, Kovács A, Muszbek L, Fésüs L (2005) High-throughput scintillation proximity assay for transglutaminase activity measurement. Anal Biochem 343 (2):256-262

Murthy SN, Lorand L (2000) Nucleotide binding by the erythrocyte transglutaminase/G_h protein, probed with fluorescent analogs of GTP and GDP. Proc Natl Acad Sci U S A 97 (14):7744-7747

Nakayama GR, Bingham P, Tan D, Maegley KA (2006) A fluorescence polarization assay for screening inhibitors against the ribonuclease H activity of HIV-1 reverse transcriptase. Anal Biochem 351 (2):260-265

Nguyen T, Francis MB (2003) Practical synthetic route to functionalized rhodamine dyes. Org Lett 5 (18):3245-3248

Odii BO, Coussons P (2014) Biological functionalities of transglutaminase 2 and the possibility of its compensation by other members of the transglutaminase family. ScientificWorldJournal 2014:714561

Owicki JC (2000) Fluorescence polarization and anisotropy in high throughput screening: perspectives and primer. J Biomol Screen 5 (5):297-306

Pardin C, Pelletier JN, Lubell WD, Keillor JW (2008) Cinnamoyl inhibitors of tissue transglutaminase. J Org Chem 73 (15):5766-5775

Pardin C, Roy I, Chica RA, Bonneil E, Thibault P, Lubell WD, Pelletier JN, Keillor JW (2009) Photolabeling of Tissue Transglutaminase Reveals the Binding Mode of Potent Cinnamoyl Inhibitors. Biochemistry 48 (15):3346-3353

Perez Alea M, Kitamura M, Martin G, Thomas V, Hitomi K, El Alaoui S (2009) Development of an isoenzyme-specific colorimetric assay for tissue transglutaminase 2 cross-linking activity. Anal Biochem 389 (2):150-156

Pheovilov PP, Sveshnikov BJ (1940) On the concentrational depolarization of the fluorescence dye-stuff solutions. J Phys USSR 3 (6):493-505

Pietsch M, Wodtke R, Pietzsch J, Löser R (2013) Tissue transglutaminase: An emerging target for therapy and imaging. Bioorg Med Chem Lett 23 (24):6528-6543

Pinkas DM, Strop P, Brunger AT, Khosla C (2007) Transglutaminase 2 undergoes a large conformational change upon activation. PLoS Biol 5 (12):e327

Piper JL, Gray GM, Khosla C (2002) High selectivity of human tissue transglutaminase for immunoactive gliadin peptides: implications for celiac sprue. Biochemistry 41 (1):386-393

Prime ME, Andersen OA, Barker JJ, Brooks MA, Cheng RKY, Toogood-Johnson I, Courtney SM, Brookfield FA, Yarnold CJ, Marston RW, Johnson PD, Johnsen SF, Palfrey JJ,

Vaidya D, Erfan S, Ichihara O, Felicetti B, Palan S, Pedret-Dunn A, Schaertl S, Sternberger I, Ebneth A, Scheel A, Winkler D, Toledo-Sherman L, Beconi M, Macdonald D, Munoz-Sanjuan I, Dominguez C, Wityak J (2012) Discovery and structure-activity relationship of potent and selective covalent inhibitors of transglutaminase 2 for Huntington's disease. J Med Chem 55 (3):1021-1046

Radek JT, Jeong JM, Murthy SN, Ingham KC, Lorand L (1993) Affinity of human erythrocyte transglutaminase for a 42-kDa gelatin-binding fragment of human plasma fibronectin. Proc Natl Acad Sci U S A 90 (8):3152-3156

Ramos SS, Vilhena AF, Santos L, Almeida P (2000) ^{1}H and ^{13}C NMR spectra of commercial rhodamine ester derivatives. Magn Reson Chem 38 (6):475-478

Reindl W, Graber M, Strebhardt K, Berg T (2009) Development of high-throughput assays based on fluorescence polarization for inhibitors of the polo-box domains of polo-like kinases 2 and 3. Anal Biochem 395 (2):189-194

Ross JA, Gilmore MA, Williams D, Aoki KR, Steward LE, Jameson DM (2011) Characterization of Förster resonance energy transfer in a botulinum neurotoxin protease assay. Anal Biochem 413 (1):43-49

Rossi A, Catani MV, Candi E, Bernassola F, Puddu P, Melino G (2000) Nitric oxide inhibits cornified envelope formation in human keratinocytes by inactivating transglutaminases and activating protein 1. J Invest Dermatol 115 (4):731-739

Schaertl S, Prime M, Wityak J, Dominguez C, Munoz-Sanjuan I, Pacifici RE, Courtney S, Scheel A, Macdonald D (2010) A profiling platform for the characterization of transglutaminase 2 (TG2) inhibitors. J Biomol Screen 15 (5):478-487

Seebach D, Dubost E, Mathad RI, Jaun B, Limbach M, Löweneck M, Flögel O, Gardiner J, Capone S, Beck AK, Widmer H, Langenegger D, Monna D, Hoyer D (2008) New open-chain and cyclic tetrapeptides, consisting of α-, β^{2}-, and β^{3}-amino-acid residues, as somatostatin mimics - A survey. Helv Chim Acta 91 (9):1736-1786

Sem DS, McNeeley PA (1999) Application of fluorescence polarization to the steady-state enzyme kinetic analysis of calpain II. FEBS Lett 443 (1):17-19

Shapiro AB, Gao N, Gu RF, Thresher J (2014) Fluorescence anisotropy-based measurement of Pseudomonas aeruginosa penicillin-binding protein 2 transpeptidase inhibitor acylation rate constants. Anal Biochem 463:15-22

Shoichet BK (2006) Interpreting steep dose-response curves in early inhibitor discovery. J Med Chem 49 (25):7274-7277

Simeonov A, Bi X, Nikiforov TT (2002) Enzyme assays by fluorescence polarization in the presence of polyarginine: study of kinase, phosphatase, and protease reactions. Anal Biochem 304 (2):193-199

Simeonov A, Jadhav A, Thomas CJ, Wang Y, Huang R, Southall NT, Shinn P, Smith J, Austin CP, Auld DS, Inglese J (2008) Fluorescence spectroscopic profiling of compound libraries. J Med Chem 51 (8):2363-2371

Slaughter TF, Achyuthan KE, Lai TS, Greenberg CS (1992) A microtiter plate transglutaminase assay utilizing 5-(biotinamido)pentylamine as substrate. Anal Biochem 205 (1):166-171

Stein RL (2011) Kinetics of enzyme action. Essential principles for drug hunters. 1st edn. John Wiley & Sons, Hoboken, N.J., p 138

Tong L, Chen Z, De Paiva CS, Beuerman R, Li DQ, Pflugfelder SC (2006) Transglutaminase participates in UVB-induced cell death pathways in human corneal epithelial cells. Invest Ophth Vis Sci 47 (10):4295-4301

Valeur B (2001) Molecular fluorescence: principles and applications. Wiley-VCH, Weinheim, p 245

van der Meer BW (2014) Förster Theory. In: Medintz I, Hildebrandt N (eds) FRET - Förster resonance energy transfer: from theory to applications. 1st edn. Wiley-VCH, Weinheim, pp 23-62

van Geel R, Debets MF, Lowik DWPM, Pruijn GJM, Boelens WC (2012) Detection of transglutaminase activity using click chemistry. Amino Acids 43 (3):1251-1263

Verderio E, Nicholas B, Gross S, Griffin M (1998) Regulated expression of tissue transglutaminase in Swiss 3T3 fibroblasts: Effects on the processing of fibronectin, cell attachment, and cell death. Exp Cell Res 239 (1):119-138

Wityak J, Prime ME, Brookfield FA, Courtney SM, Erfan S, Johnsen S, Johnson PD, Li M, Marston RW, Reed L, Vaidya D, Schaertl S, Pedret-Dunn A, Beconi M, Macdonald D, Munoz-Sanjuan I, Dominguez C (2012) SAR development of lysine-based irreversible inhibitors of transglutaminase 2 for Huntington's disease. ACS Med Chem Lett 3 (12):1024-1028

Wu YW, Tsai YH (2006) A rapid transglutaminase assay for high-throughput screening applications. J Biomol Screen 11 (7):836-843

Yamada K, Meguro T (1977) New assay method for factor XIII using a fluorescence polarization analyzer, based on change in rotary Brownian-motion. Thromb Res 11 (5):557-566

Yamane A, Fukui M, Sugimura Y, Itoh M, Alea MP, Thomas V, El Alaoui S, Akiyama M, Hitomi K (2010) Identification of a preferred substrate peptide for transglutaminase 3 and detection of in situ activity in skin and hair follicles. FEBS J 277 (17):3564-3574

Zhang JH, Chung TDY, Oldenburg KR (1999) A simple statistical parameter for use in evaluation and validation of high throughput screening assays. J Biomol Screen 4 (2):67-73

Supplementary material for the Original Article entitled

A fluorescence anisotropy-based assay for determining the activity of tissue transglutaminase

To be published in Amino Acids

Christoph Hauser, Robert Wodtke, Reik Löser, Markus Pietsch

Christoph Hauser, Markus Pietsch
Center of Pharmacology, Medical Faculty, University of Cologne, Gleueler Str. 24, D-50931 Cologne, Germany

Robert Wodtke, Reik Löser
Helmholtz-Zentrum Dresden-Rossendorf, Institute of Radiopharmaceutical Cancer Research, Bautzner Landstr. 400, D-01328 Dresden, Germany
and
Department of Chemistry and Food Chemistry, Technical University Dresden, Mommsenstraße 4, D-01062 Dresden, Germany

Christoph Hauser and Robert Wodtke as well as Reik Löser and Markus Pietsch contributed equally to this study.

Corresponding authors
Dr. Markus Pietsch, Center of Pharmacology, Medical Faculty, University of Cologne, Gleueler Str. 24, D-50931 Cologne, Germany, Phone: +49 (0)221 478-97737, Fax: +49 (0)221 478-5022, E-Mail: markus.pietsch@uk-koeln.de

Dr. Reik Löser, Helmholtz-Zentrum Dresden-Rossendorf, Institute of Radiopharmaceutical Cancer Research, Bautzner Landstr. 400, D-01328 Dresden, Germany, Phone: +49 (0)351 260-3658, Fax: +49 (0)351 260-2915, E-Mail: r.loeser@hzdr.de

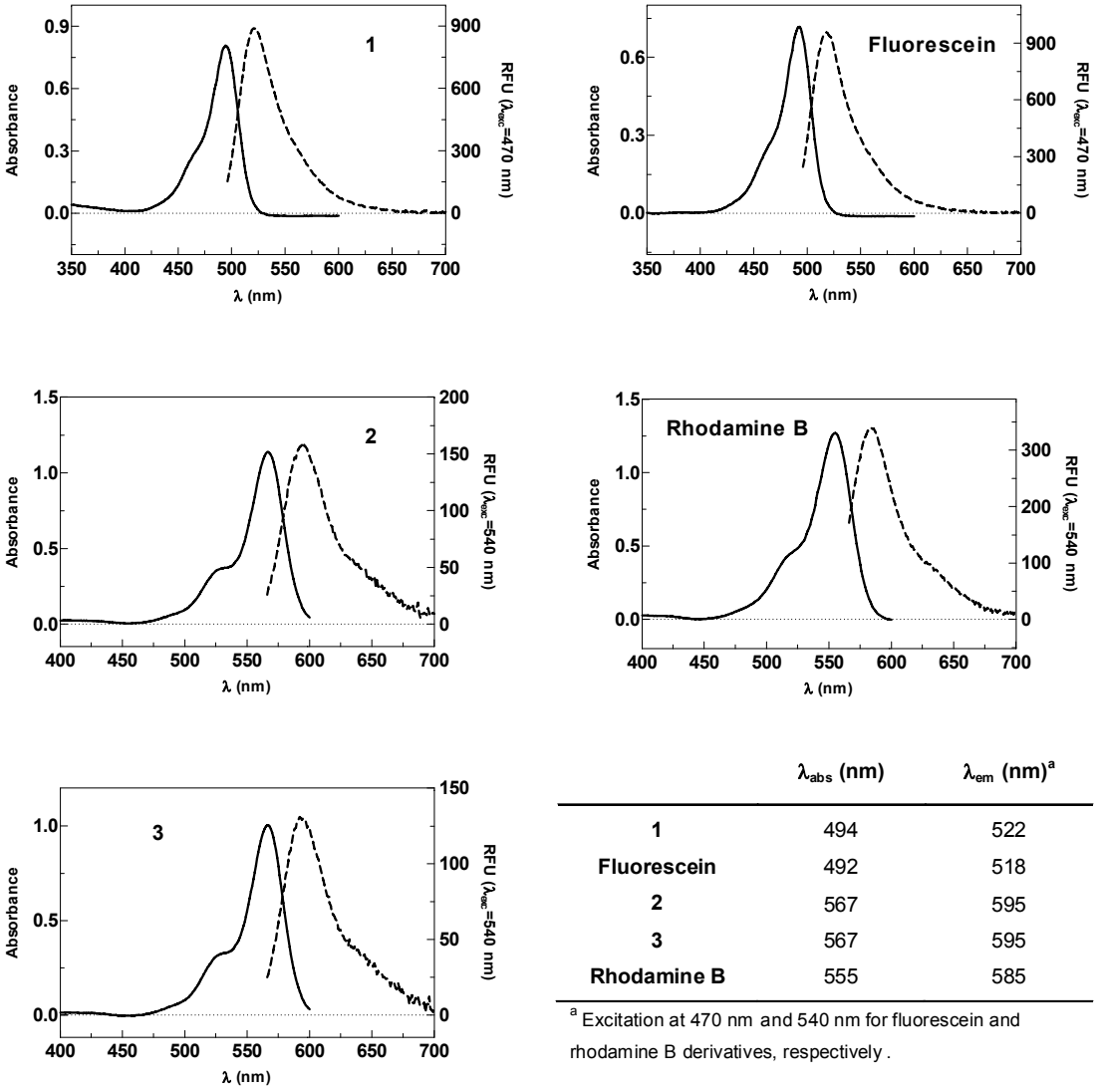

	λ_{abs} (nm)	λ_{em} (nm)[a]
1	494	522
Fluorescein	492	518
2	567	595
3	567	595
Rhodamine B	555	585

[a] Excitation at 470 nm and 540 nm for fluorescein and rhodamine B derivatives, respectively.

Fig. S1 Absorption spectra (solid lines) and emission spectra (dashed lines) of the compounds **1-3** and the isolated fluorophores fluorescein and rhodamine B in MOPS assay buffer pH 8.0 containing 5% DMSO. Absorption spectra were recorded at a compound concentration of 10 µM. Emission spectra were recorded at either 4 µM (fluorescein and its derivative) or 10 µM (rhodamine B and its derivatives). All spectra were corrected by the absorption or the emission in the absence of the fluorescent compound. Wavelengths of maximum absorption and emission are summarized in the table

NMR spectra of compounds 1-3

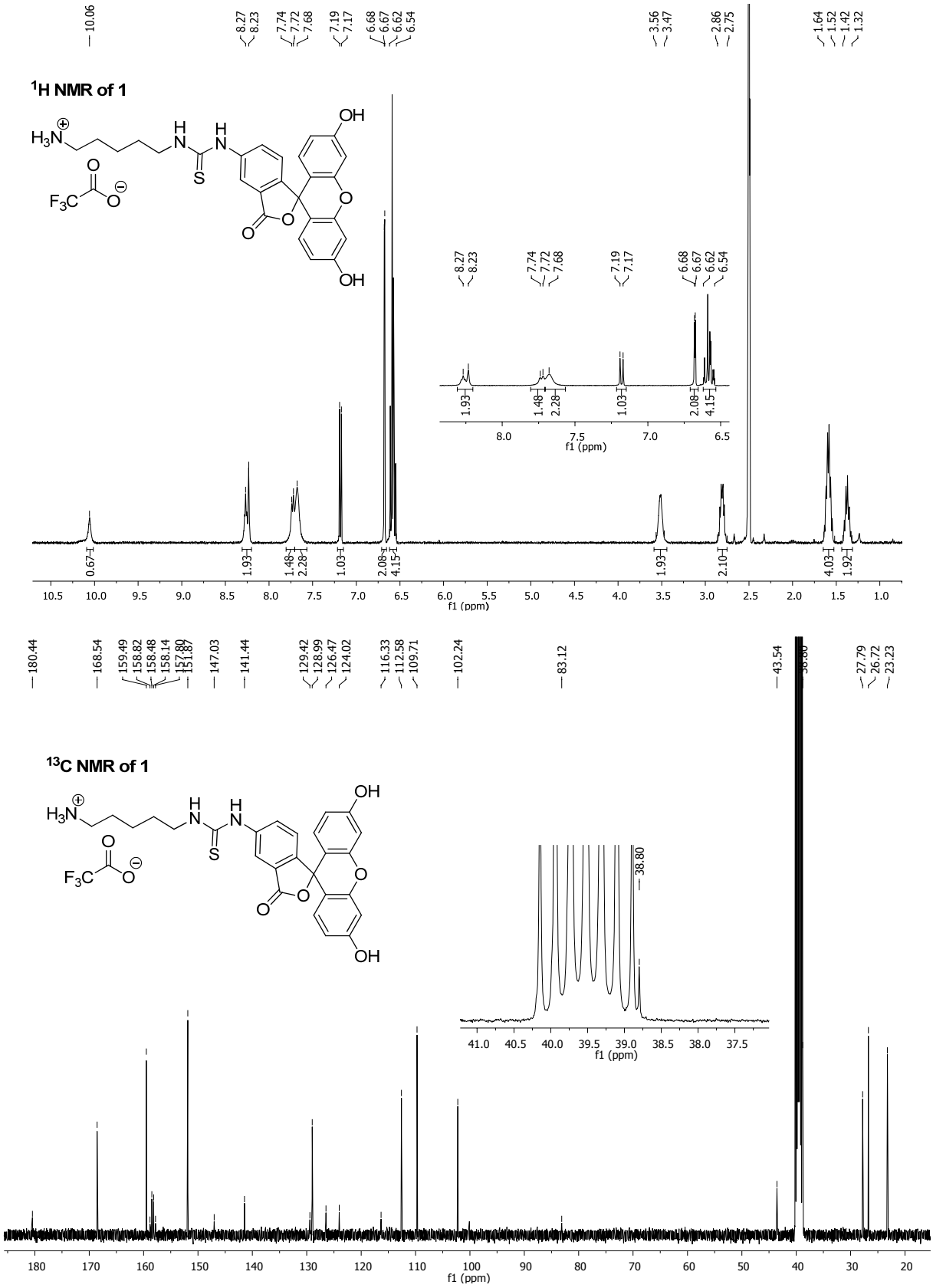

Fig. S2 ^{1}H NMR (top) and ^{13}C NMR (bottom) spectra of compound **1**

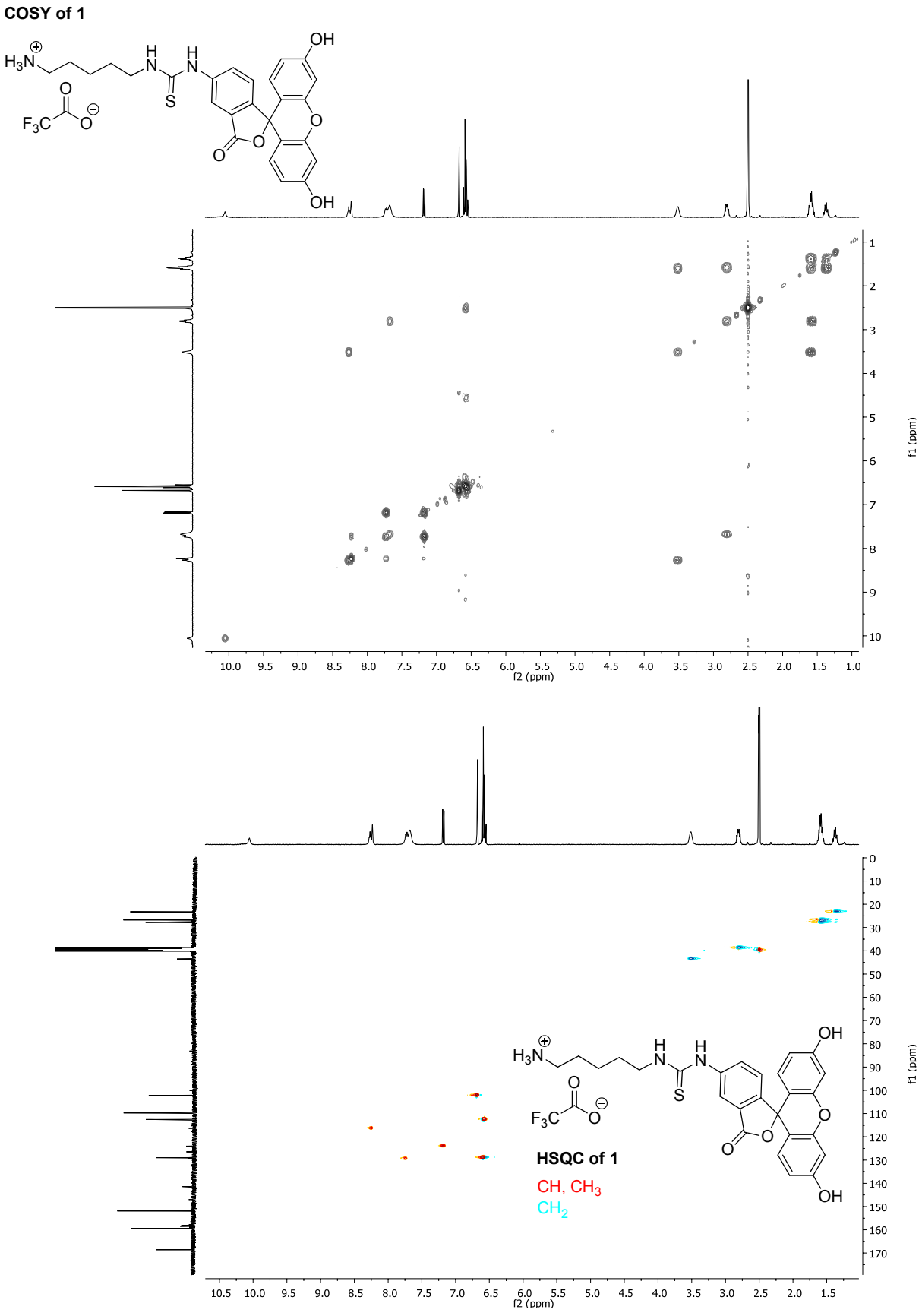

Fig. S3 2D ^{1}H,^{1}H COSY (top) and ^{13}C,^{1}H HSQC (bottom) spectra of compound **1**

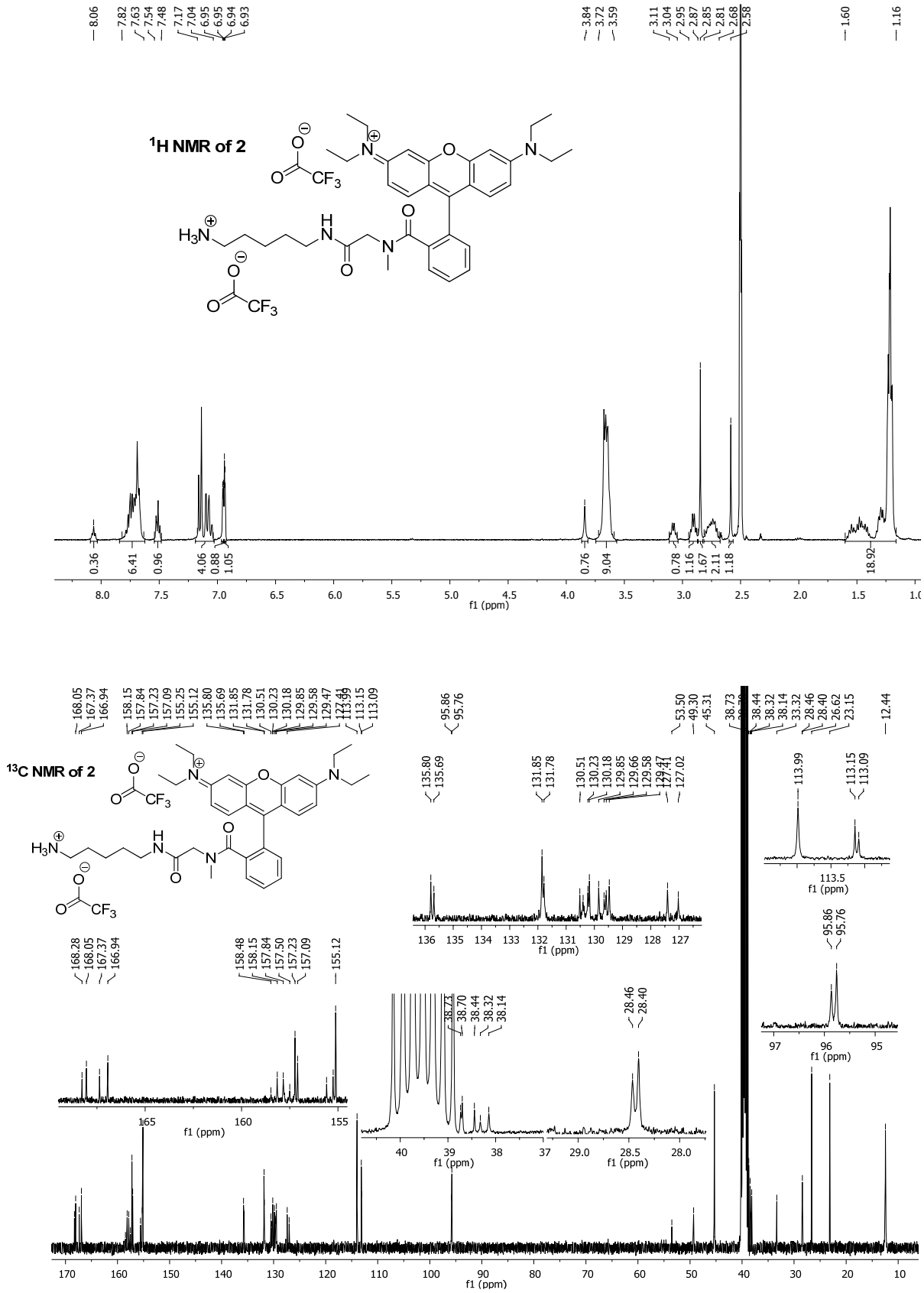

Fig. S4 ^{1}H NMR (top) and ^{13}C NMR (bottom) spectra of compound **2**

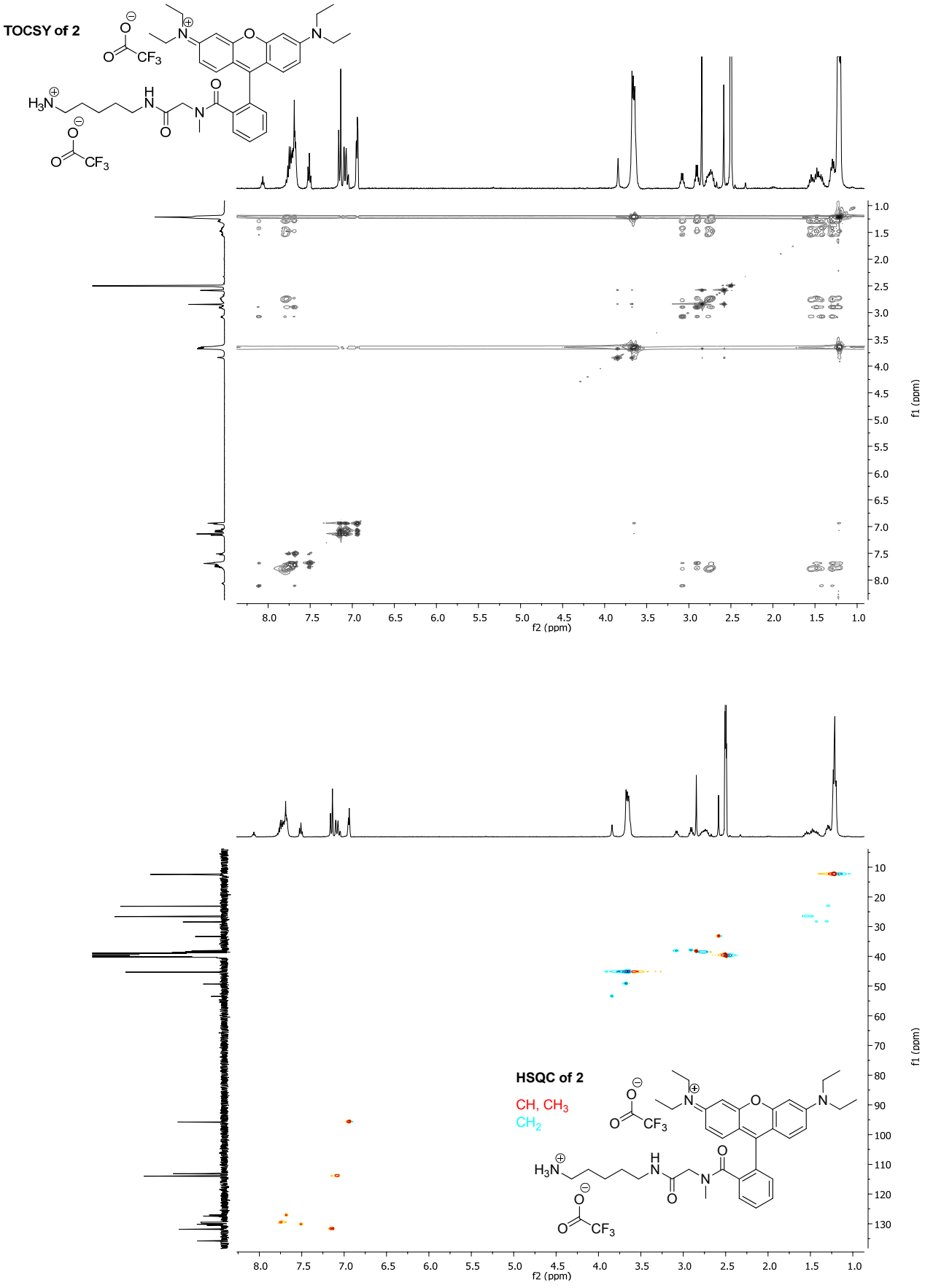

Fig. S5 2D ^{1}H,^{1}H TOCSY (top) and ^{13}C,^{1}H HSQC (bottom) spectra of compound **2**

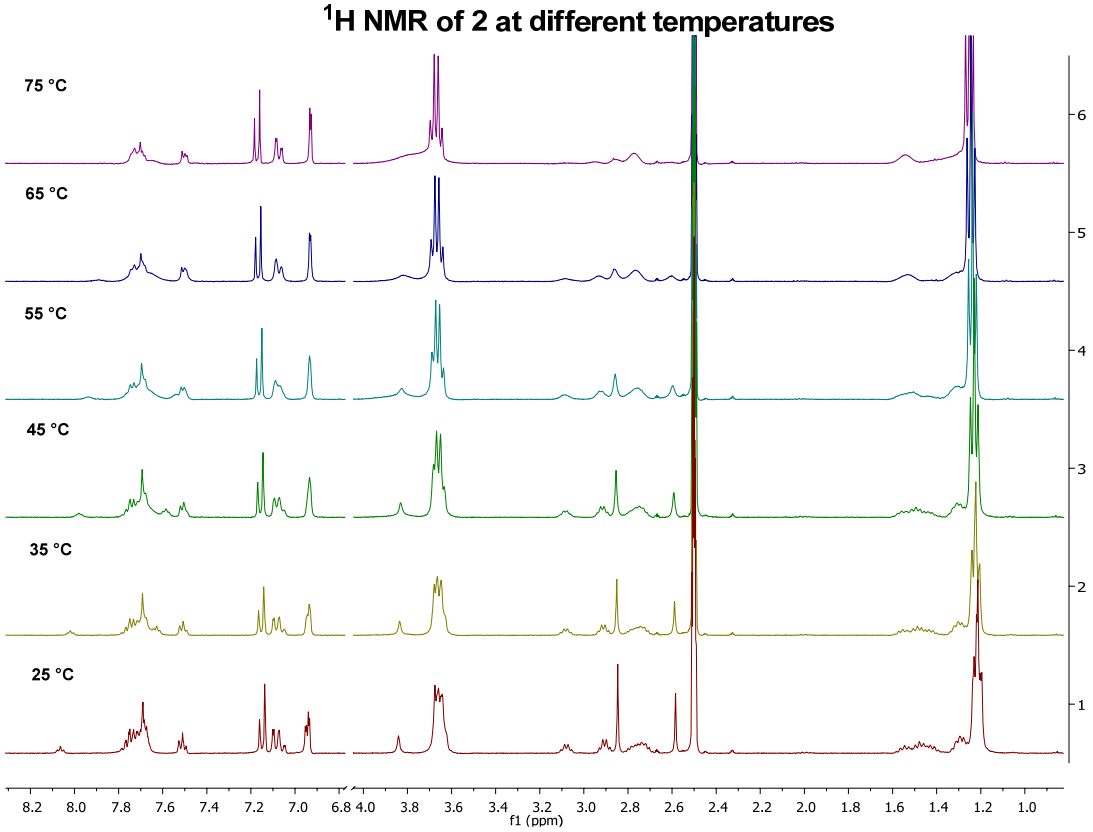

Fig. S6 ^{1}H NMR spectra of compound **2** obtained at different temperatures

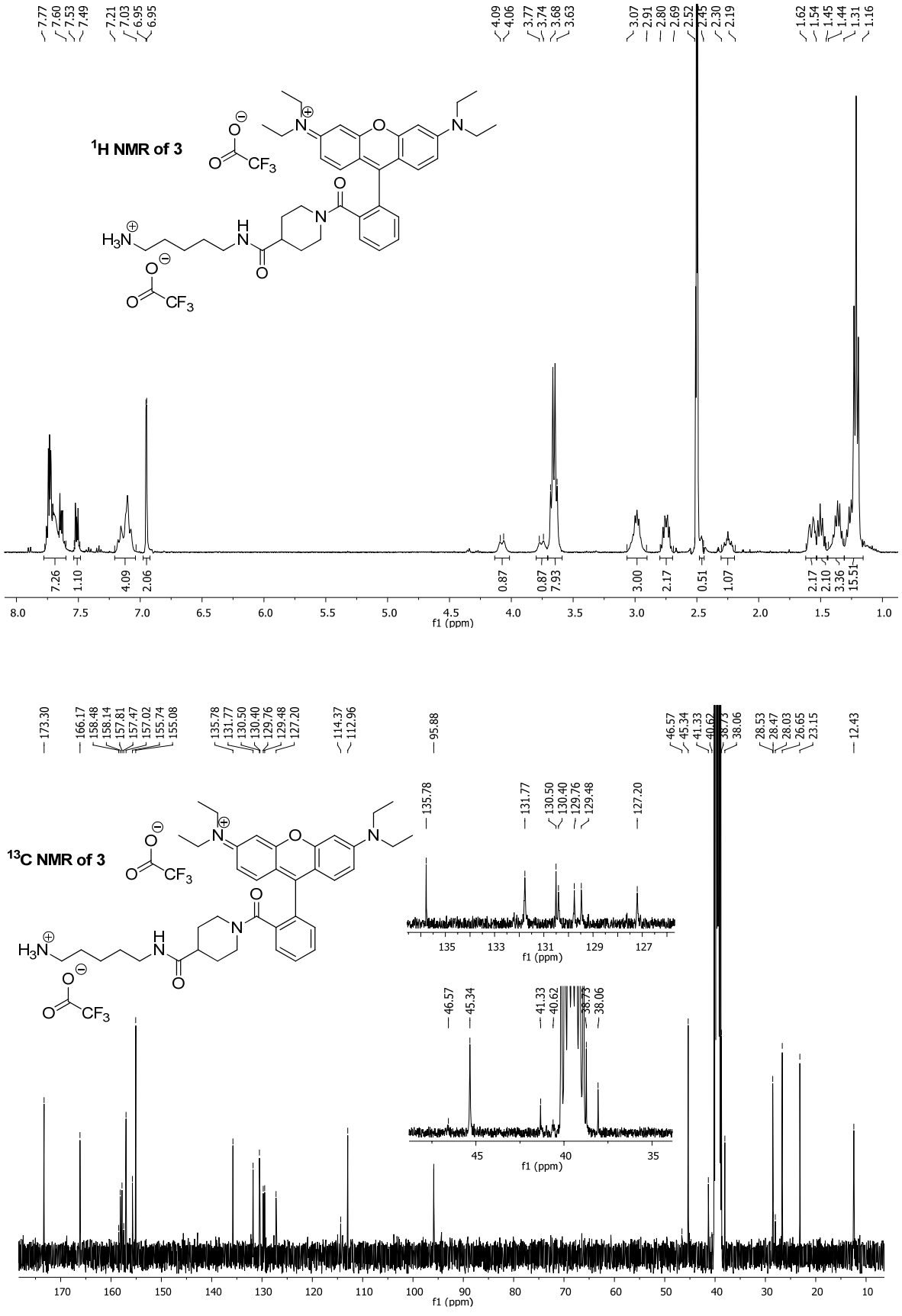

Fig. S7 ^{1}H NMR (top) and ^{13}C NMR (bottom) spectra of compound **3**

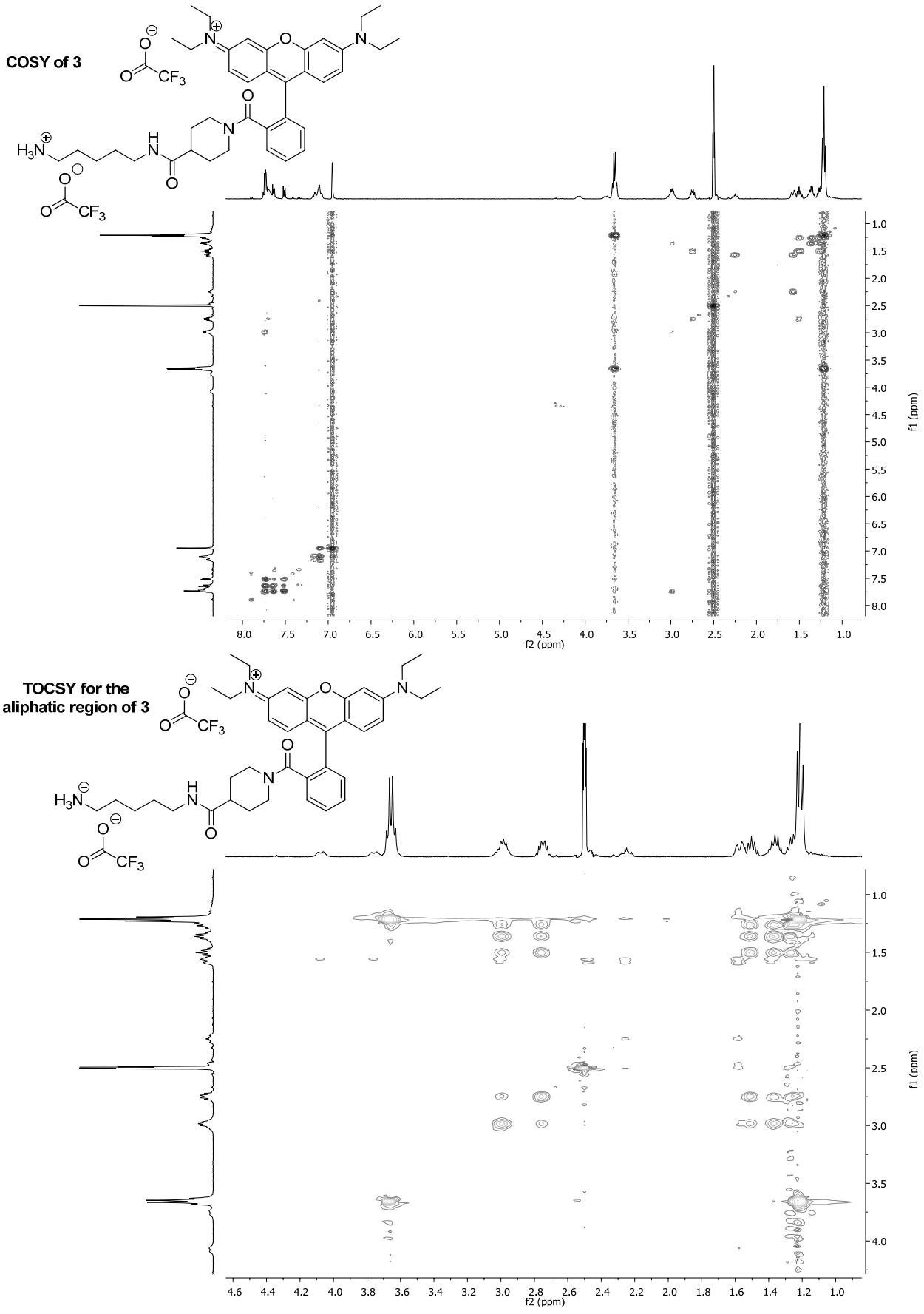

Fig. S8 2D $^{1}H,^{1}H$ COSY (top) and $^{1}H,^{1}H$ TOCSY (bottom) spectra of compound **3**

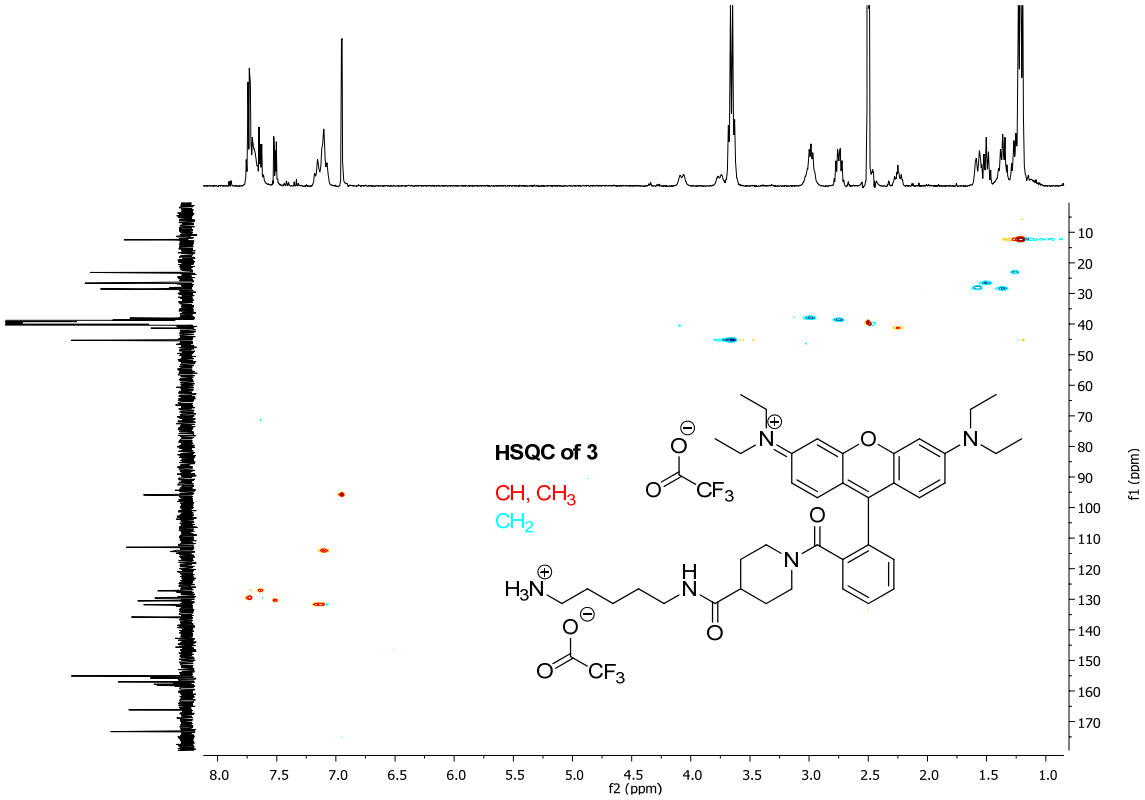

Fig. S9 2D $^{13}C,^{1}H$ HSQC spectrum of compound **3**

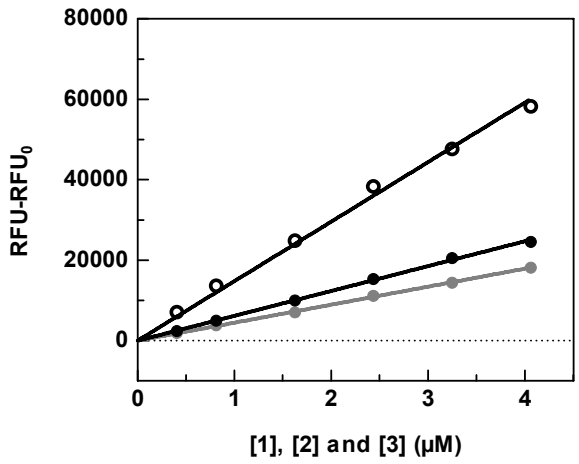

Fig. S10 Plots of the fluorescence versus the concentration of **1** (black open symbols), **2** (grey filled symbols), and **3** (black filled symbols), respectively. Data shown are mean values ± SEM of 3 separate experiments, each performed in triplicate. The sensitivity of the plate reader was set to 35. Values of fluorescence were corrected by those obtained in the absence of **1**, **2**, and **3**, respectively, and analyzed by linear regression forced through the origin. Slopes (mean values ± SEM, n = 3) obtained were 14798 ± 166 RFU μM^{-1} (**1**), 4477 ± 19 RFU μM^{-1} (**2**), 6169 ± 211 RFU μM^{-1} (**3**)

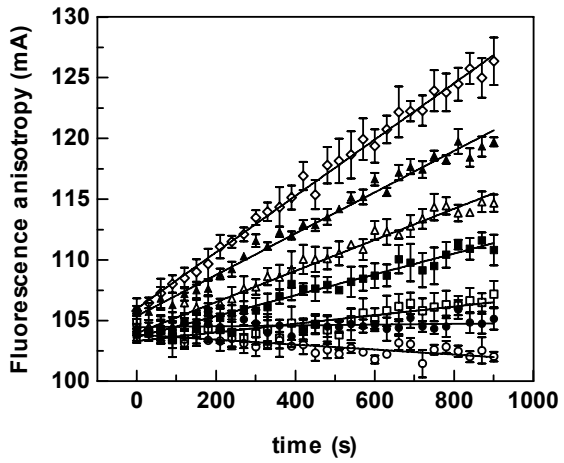

Fig. S11 Plots of the FA over time for the reaction of **2** (0.81 μM) with DMC (10 μM) in the absence of gpTGase 2 (open circles) and in the presence of various concentrations of gpTGase 2: filled circles, 0.5 μg/mL; open squares, 1 μg/mL; filled squares, 2 μg/mL; open triangles, 3 μg/mL; filled triangles, 4 μg/mL; open rhombi, 5 μg/mL. Data shown are mean values ± SEM of three separate experiments, each performed in duplicate or triplicate. Analysis was done by linear regression

a)

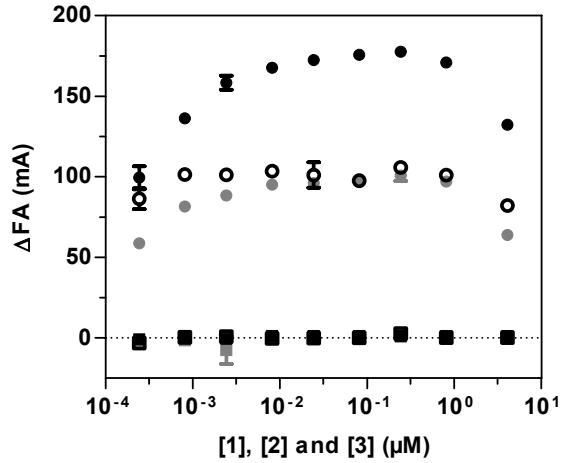

b)

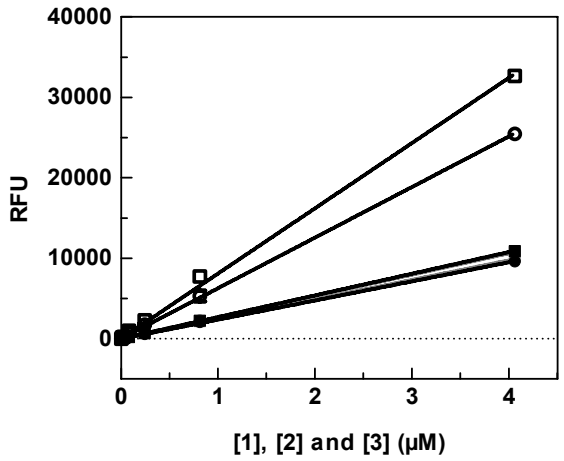

Fig. S12 Plots of the change in fluorescence anisotropy over the course of the reaction (0-3 h) (a) and the fluorescence intensity obtained after 3 h, i.e. at the time of completed conversion (b) versus the acyl acceptor concentration for the reaction of DMC (**1**, **2**: 10 µM; **3**: 30 µM) with **1** (black open symbols), **2** (grey filled symbols), and **3** (black filled symbols), respectively, in the presence (circles) and absence (squares) of gpTGase 2 (5 µg/mL). Data points are mean values ± SD of a single experiment performed with one or two replicates. Data in (b) were subjected to linear regression analysis.

a)

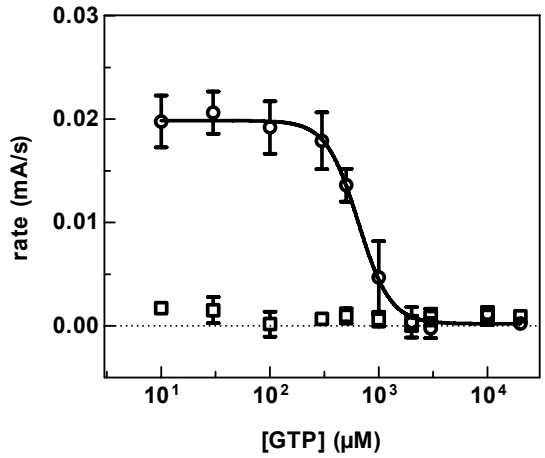

b)

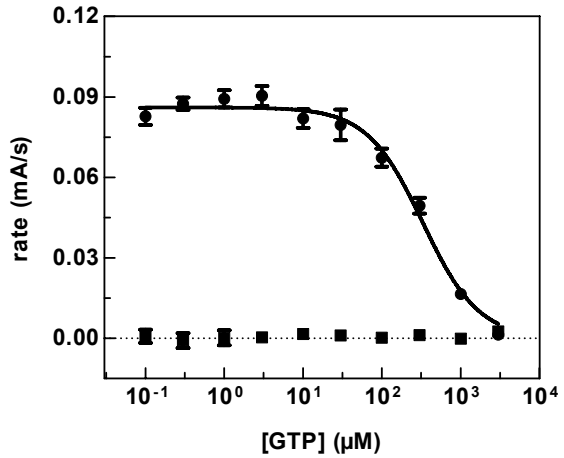

Fig. S13 Inhibition of gpTGase 2 (5 µg/mL) by GTP. Data shown for the reaction in the presence (circles) and absence (squares) of enzyme are mean values ± SEM of 3 separate experiments, each performed in duplicate or triplicate. a) Determination was done with the substrates DMC (10 µM) and **1** (0.81 µM) in MOPS assay buffer pH 8.0. Analysis by non-linear regression gave the following values (mean values ± SEM): IC_{50} = 691 ± 111 µM, n_H = -4.44 ± 1.63 (n_H is not significantly different from one, One-sample t-test, $P > 0.05$). b) Determination was done with the substrates DMC (30 µM) and **3** (0.81 µM) in HEPES assay buffer pH 7.4. Analysis by non-linear regression gave the following values (mean values ± SEM): IC_{50} = 329 ± 20 µM, n_H = -1.22 ± 0.08 (Bottom was set to 0, n_H is not significantly different from one, One-sample t-test, $P > 0.05$)

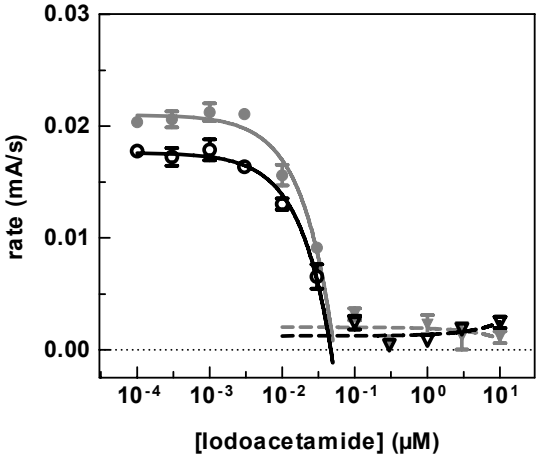

Fig. S14 Active site titration of gpTGase 2 (5 µg/mL) using the inhibitor iodacetamide and the substrates DMC (10 µM) and compound **1** (0.81 µM, black open symbols) or DMC (10 µM) and compound **2** (0.81 µM, grey filled symbols). Data shown for the reaction in the presence of enzyme are taken from Fig. 4a and represent mean values ± SEM of 2-3 separate experiments, each performed in triplicate. Active enzyme concentrations (Mean ± SD) of 43.9 ± 5.6 nM and 47.0 ± 2.7 nM, i.e. 67.3 ± 8.6% and 72.0 ± 4.2% active gpTGase 2 with regards to the total protein concentration, were calculated for the experiments in the presence of compounds **1** and **2**, respectively. The amounts of active gpTGase 2 are not significantly different (One-sample t-test, $P > 0.05$) from the content calculated on the basis of activity data obtained by the hydroxamate assay (Folk and Cole 1966), which were provided by Zedira, Darmstadt, Germany

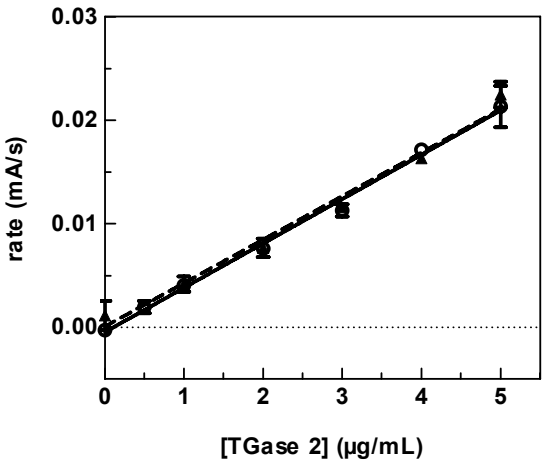

Fig. S15 Plots of the rate versus the gpTGase 2 concentration for the reaction of DMC (10 µM) with **1** (0.81 µM). Data of isolated gpTGase 2 (open circles, same as in Fig. 2) and recombinant gpTGase 2 (filled triangles) shown are mean values ± SEM of 3-4 separate experiments, each performed in triplicate. Analysis by linear regression gave slopes (mean values ± SEM) of 0.00424 ± 0.00020 mA mL s^{-1} μg^{-1} (n = 4, full line, same as in Fig. 2) for isolated TGase 2 and 0.00415 ± 0.00018 mA mL s^{-1} μg^{-1} (n = 3, dashed line) for the recombinant enzyme, with the two slopes being not significantly different (unpaired two sample Student's t test, $P > 0.05$)

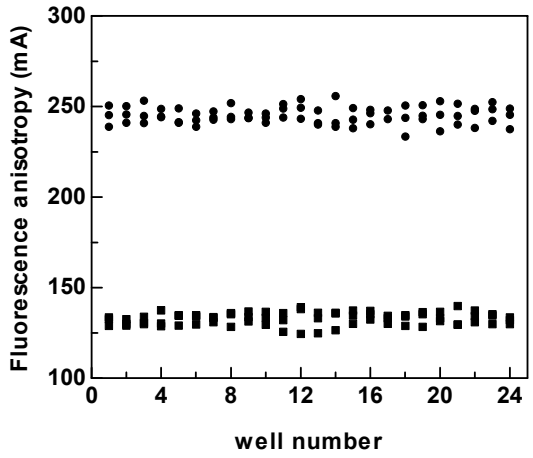

Fig. S16 Determination of the Z' factor for the reaction of DMC (30 µM) with cadaverine derivative **3** (0.81 µM) catalyzed by recombinant guinea pig liver TGase 2 (5 µg/mL) in the absence (circles) and presence (squares) of iodoacetamide (10 µM). FA values from three separate experiments obtained at the end of the kinetic measurement after 15 min are shown, with 23-24 wells being used for each of the two conditions per experiment. A Z' factor of 0.863 ± 0.003 (mean ± SEM, n = 3) was calculated by applying the equation $Z' = 1 - [(3SDFA_{free} + 3SDFA_{inhibited})/(|meanFA_{free} - meanFA_{inhibited}|)]$ to each experiment, where SD and mean are the standard deviations and mean values of the FA, respectively, of those wells containing either the free gpTGase 2 or the fully inhibited enzyme (Zhang et al. 1999). The so obtained Z' factor is not significantly different from the value calculated from the kinetic experiments shown in Fig. 4b (paired two sample Student's t test, $P > 0.05$)

References

Folk JE, Cole PW (1966) Transglutaminase: mechanistic features of the active site as determined by kinetic and inhibitor studies. Biochim Biophys Acta 122 (2):244-264

Zhang JH, Chung TDY, Oldenburg KR (1999) A simple statistical parameter for use in evaluation and validation of high throughput screening assays. J Biomol Screen 4 (2):67-73